Nonreciprocal charge transport in two-dimensional noncentrosymmetric superconductors

Shintaro Hoshino,[1] Ryohei Wakatsuki,[2] Keita Hamamoto,[2] and Naoto Nagaosa[3,2]
[1]*Department of Physics, Saitama University, Shimo-Okubo 255, Sakura-ku, Saitama 338-8570, Japan*
[2]*Department of Applied Physics, University of Tokyo, Hongo 7-3-1, Bunkyo-ku, Tokyo 113-8656, Japan*
[3]*RIKEN Center for Emergent Matter Science (CEMS), Wako, Saitama 351-0198, Japan*

(Received 16 May 2018; revised manuscript received 31 July 2018; published 20 August 2018)

Nonreciprocal charge transport phenomena are studied theoretically for two-dimensional noncentrosymmetric superconductors under an external magnetic field B. Rashba superconductors, surface superconductivity on the surface of three-dimensional topological insulators, and transition-metal dichalcogenides such as MoS_2 are representative systems, and the current-voltage I-V characteristics, i.e., $V = V(I)$, for each of them is analyzed. $V(I)$ can be expanded with respect to the current I as $V(I) = \sum_{j=1,\infty} a_j(B, T)I^j$, and the (B, T) dependence of a_j depends on the mechanism of the charge transport. Our analysis is based on the time-dependent Ginzburg-Landau theory, which contains up to third-order terms in the momentum of the order parameter. Above the mean field superconducting transition temperature T_0, the fluctuation of the superconducting order parameter gives the additional conductivity, i.e., paraconductivity. With the extension of paraconductivity to the nonlinear response, we obtain the nonreciprocal charge transport. On the other hand, below T_0, the vortices determine the Kosterlitz-Thouless transition and also the resistivity. The nonreciprocal resistivity is analyzed from the dynamics of vortices in this temperature region. Based on these results, we propose the experiments to identify the mechanism of the nonreciprocal transport with the realistic estimates for the order of magnitude of the coefficients $a_j(B, T)$ for each case.

DOI: 10.1103/PhysRevB.98.054510

I. INTRODUCTION

The nonreciprocal charge transport in noncentrosymmetric systems is a fundamental and important issue. It is deeply related to the broken symmetry of spatial inversion P and the time reversal T. For the linear response, the microscopic time-reversal symmetry leads to the Onsager's reciprocal theorem [1,2] given by

$$K_{AB}(q, \omega, B) = \epsilon_A \epsilon_B K_{BA}(-q, \omega, -B), \tag{1}$$

where $K_{AB}(q, \omega, B)$ describes the linear response of the physical observable A to the field coupled to the observable B with the wave vector q and frequency ω under the magnetic field B (which breaks the time-reversal symmetry). $\epsilon_A = \pm 1$ (ϵ_B) specifies the even (1) or odd (-1) nature of the observable A (B) with respect to T. On the other hand, the spatial inversion symmetry gives

$$K_{AB}(q, \omega, B) = \eta_A \eta_B K_{AB}(-q, \omega, B), \tag{2}$$

with η_A (η_B) being the analogous quantity to $\epsilon_A = \pm 1$ (ϵ_B) for P. When both of T and P are broken, the Onsager reciprocal theorem allows the directional linear response of the diagonal response. For example, the dielectric function for light can have the form $\varepsilon_{\mu\mu}(q, \omega, B) = \varepsilon_0 + \alpha B q$ which describes the directional dichroism of unpolarized light.

Rikken extended this consideration to the nonlinear response by heuristic argument, i.e., replacing the wave vector q by the current I, leading to the expression of the resistivity [3,4]

$$R = R_0(1 + \gamma B I). \tag{3}$$

The coefficient γ, which is called γ value in the following, is usually a rather small value of the order of $\sim 10^{-2}$ to 10^{-1} T^{-1} A^{-1} [5–8]. This is because the nonreciprocal transport requires both the magnetic energy $\mu_B B$ and the spin-orbit interaction λ, which are small compared with the energy denominator, i.e., kinetic energy of the electrons (typically the Fermi energy E_F). To enhance the nonreciprocal transport, there are two ways. One is to reduce the energy denominator and the other is to enlarge the spin-orbit interaction. This is realized in BiTeBr with the giant bulk Rashba splitting by reducing the electron density [9]. Furthermore, in the superconductors, the Fermi energy is replaced by the energy gap in the energy denominator, which leads to the huge enhancement of γ as demonstrated in MoS_2 [10]. The theoretical analysis, however, is limited to the paraconductivity above the mean field transition temperature T_0, and that below T_0 still remains an important unresolved issue although the experiment shows the further increasing value of γ there [10].

In this paper, we give a comprehensive and unified treatment of the nonreciprocal charge transport in two-dimensional noncentrosymmetric superconductors (2DNS). There are several possible mechanisms for it, and accordingly we generalize Eq. (3) to the current (I)-voltage (V) characteristics as

$$V(I) = \sum_{j=1}^{\infty} a_j(B, T)I^j. \tag{4}$$

We take (i) the Rashba superconductors, and surface superconductivity on the surface of three-dimensional topological insulators (TIs), and (ii) the transition-metal dichalcogenides

TABLE I. Summary of nonreciprocal charge transport in two-dimensional noncentrosymmetric superconductors at low magnetic field B. The parameters are electron charge e and band mass m, Fermi energy $E_{\rm F}$, Fermi velocity $v_{\rm F}$, Rashba parameter α (we also define $E_{\rm FR} = 2E_{\rm F} + m\alpha^2$), triplet or singlet pair mixing parameter $r_{\rm t,s}$, cutoff energy $E_{\rm c}$, hexagonal or trigonal warping parameter λ, spin-orbit splitting $\Delta_{\rm SO}$, mean field superconducting transition temperature T_0, and Kosterlitz-Thouless transition temperature $T_{\rm KT}$. The unit system $\hbar = k_{\rm B} = \mu_{\rm B} = 1$ is used. The sample width W is omitted from the expressions. The temperature dependence for the paraconductivity contributions at $T > T_0$ enters through the formula in Eq. (6). See each section for more details.

		Rashba SC $(B \perp \hat{z})$	TI surface + SC $(B \perp \hat{z})$		TMD $(B \parallel \hat{z})$
Symmetry		C_∞		Hexagonal	Trigonal
$T > T_0$	Normal	$V = a_1 I(1 + \gamma_{\rm N} BI)$			
		[Sec. II A] $\gamma_{\rm N} = 0$ $(E_{\rm F}>0)$ $\gamma_{\rm N} \sim \frac{\alpha}{e(m\alpha^2 E_{\rm FR})^{3/2}}$ $(E_{\rm F}<0)$	[Sec. II B 1] $\gamma_{\rm N} \sim \frac{\mathrm{sgn}\, E_{\rm F}}{emv_{\rm F}E_{\rm F}^2}$	[Sec. II B 2] $\gamma_{\rm N} \sim \frac{\lvert E_{\rm F}\rvert\lambda}{ev_{\rm F}^5}$	[Sec. II C] $\gamma_{\rm N} \sim \frac{m\Delta_{\rm SO}\lambda}{eE_{\rm F}^3}$
	Paraconductivity	$V = a_1 I(1 + \gamma_{\rm S} BI)$			
		Parity mixing $(E_{\rm F}>0)$ $\gamma_{\rm S} \sim \frac{r_{\rm t,s}E_{\rm F}\alpha}{eT_0^3 E_{\rm FR}\ln(E_{\rm c}/T_0)}$ $\boldsymbol{q}$-cubic term $(E_{\rm F}<0)$ $\gamma_{\rm S} \sim \frac{1}{em\alpha E_{\rm FR}T_0}$	$\gamma_{\rm S} \sim \frac{1}{emv_{\rm F}E_{\rm F}T_0}$	$\gamma_{\rm S} \sim \frac{E_{\rm F}^2\lambda}{ev_{\rm F}^5 T_0}$	$\gamma_{\rm S} \sim \frac{m\Delta_{\rm SO}\lambda}{eT_0^3}$
$T < T_0$		KT transition			No KT transition
		$T_{\rm KT} < T < T_0$	[Sec. III A] $V = a_1 I(1 + \gamma_{\rm S} BI)$ $\gamma_{\rm S} \sim (T_0 - T)^{-1}$ $(T \to T_0)$ $\gamma_{\rm S} \sim (T - T_{\rm KT})^{-3/2}$ $(T \to T_{\rm KT})$		*Viscous vortex flow* [Sec. III A,B] $V = a_1' BI(1 + \gamma_{\rm S} BI)$ $\gamma_{\rm S} \sim \frac{m\Delta_{\rm SO}\lambda}{eT_0 E_{\rm F}(T_0 - T)}$
		$T < T_{\rm KT}$	$V = a_3 I^3 + a_4' BI^4$		*Ratchet mechanism* [Sec. III C] $V = a_1' BI(1 + \gamma_{\rm S}' I)$

(TMD) such as MoS_2, as the two representative examples of 2DNS.

In 2D superconductors, there are two characteristic temperatures. One is the mean field transition temperature T_0, below which the amplitude of the order parameter develops, and the other is the Kosterlitz-Thouless (KT) transition temperature $T_{\rm KT}$, below which the vortices and antivortices are bound and the resistivity becomes zero. The behavior of the resistivity $R(T)$ as a function of the temperature is well described by

$$R(T) \cong 2.7R_n[\xi_c/\xi_+(T)]^2, \tag{5}$$

with R_n being the normal-state resistivity and $\xi_+(T)$ is the diverging coherence length $\xi_+(T) = \xi_c b^{-1/2}\sinh[(b\tau_c/\tau)^{1/2}]$ where the reduced temperatures are introduced by $\tau = (T - T_{\rm KT})/T_{\rm KT}$ and $\tau_c = (T_0 - T_{\rm KT})/T_{\rm KT}$ [11]. The parameter ξ_c is a coherence length obtained by the GL theory and b is an order of unity constant. With the external magnetic field B, the situation depends on its direction. With the in-plane B, only the Zeeman effect is relevant, and KT transition survives with the reduced transition temperature $T_{\rm KT}(B)$. This is the case for (i) to obtain the nonreciprocal transport. On the other hand, with the out-of-plane magnetic field considered in the case (ii), the vortices are introduced even below $T_{\rm KT}$, and the system remains resistive down to low temperatures. The experiment for MoS_2 [10] employs this configuration, and continues to define γ in Eq. (3), although the B dependence of $a_2(B, T)$ is different for different mechanisms as shown below.

The obtained results for nonreciprocal charge transport are summarized in Table I, which will be discussed in greater detail in the rest of this paper. Our plan is as follows. In Sec. II, we study the paraconductivity above the mean field transition temperature T_0 in terms of the Ginzburg-Landau theory derived for several cases of interest. In Sec. III we present the analysis of the charge transport below T_0, where the vortex motion is responsible for the voltage under the current flow. There are three mechanisms for the nonreciprocal response, i.e., (i) the change in the KT transition temperature due to the current, (ii) the modified dissipation for the vortex motion due to the current, and (iii) the Ratchet potential for the vortex. Sections IV and V are devoted to the discussion and conclusions, respectively. The detailed derivation of GL free energy is given in Appendix A. Appendices B and C describe the effects of impurity and Landau levels, respectively, for TMD.

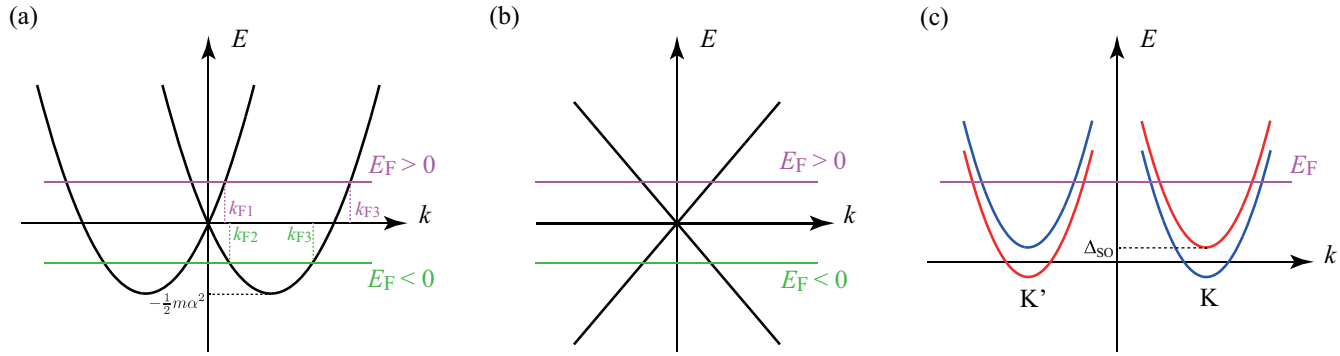

FIG. 1. Schematic illustrations for the dispersion relations in (a) Rashba system [Eq. (7)], (b) TI surface [Eq. (39)], and (c) TMD [Eq. (57)]. Here, we consider the normal states without magnetic field.

II. GINZBURG-LANDAU THEORY AND PARACONDUCTIVITY IN NONCENTROSYMMETRIC SUPERCONDUCTORS

We discuss the nonreciprocal current in the temperature regime slightly above the mean field critical temperature ($T \gtrsim T_0$). In this regime, the charge current is mainly carried by the thermal fluctuation of the superconducting order parameter. Such excess conductivity is called paraconductivity [12,13]. The paraconductivity consists of the Aslamazov-Larkin (AL) contribution [14] and the Maki-Thompson (MT) contribution [15,16]. Although fully quantum treatment is necessary for the MT term, the AL term can be discussed by the Ginzburg-Landau (GL) theory [12,13,17].

The nonreciprocity of the paraconductivity has been studied in two-dimensional TMD [10] and Rashba systems [18]. It is expected that the MT term is smaller than the AL term under a magnetic field due to pair-breaking effect [19] by external field, and the explicit forms of the γ values in Eq. (3) have been calculated based on the GL theory. Two different origins of the nonreciprocal current have been discussed in these materials, i.e., the trigonal warping of the band structure in the TMD [10], and the parity mixing of the singlet and triplet order parameters [20,21] in the superconducting Rashba systems. In both of the systems, the nonreciprocity is markedly enhanced in the superconducting fluctuation regime because of the scale difference between the Fermi energy and the superconducting gap.

In this section, we discuss the nonreciprocal paraconductivity in five models: the Rashba superconductors with and without parity mixing, the surface state of topological insulator with the parabolic dispersion and the hexagonal warping, and the two-dimensional TMD [10]. We will also compare these results with the normal contribution to demonstrate the enhancement of nonreciprocal signal in the superconducting fluctuation regime. While some of the results in the following are not entirely new as they have been published previously [9,10,18], here we have briefly provided them again in order to make this paper self-contained and complete.

In the following of this section, we derive an expression for the γ value in the region where the paraconductivity dominates over the normal conductivity near the mean field temperature T_0. With the paraconductivities defined by $j = \sigma_1 E + \sigma_2 E^2$ where j is a current density and E is an electric field, the γ value in Eq. (3) is given by $\gamma_S = \sigma_2/B\sigma_1^2 W$ with the sample width W. Since the temperature dependencies are $\sigma_1(T) \propto (T - T_0)^{-1}$ and $\sigma_2(T) \propto (T - T_0)^{-2}$ as shown later, γ_S is T independent. The deviation from the $T \to T_0$ limit can be included by the replacement $\sigma_1(T) \to \sigma_1(T) + \sigma_n$ where σ_n is a normal conductivity. Then, the temperature dependence for $\gamma_S(T) \propto \sigma_2(T)/[\sigma_1(T) + \sigma_n]^2$ enters as

$$\gamma_S(T) = \gamma_S\left[1 + \frac{1}{c_0}\frac{\sigma_n}{e^2/h}\frac{T - T_0}{T_0}\right]^{-2}, \tag{6}$$

where c_0 is a constant and h is a Planck constant. This formula is relevant for the wider temperature range. The detailed functional form of γ_S in the right-hand side of Eq. (6) can be found in the rest of this section.

A. Rashba superconductor

1. Parity mixing

In the following of this paper, we use the unit system $\hbar = k_B = \mu_B = 1$ unless otherwise specified explicitly. In Ref. [18], the nonreciprocal current due to the parity mixing of the superconducting order parameter has been studied in the Rashba superconductors. The normal-state Hamiltonian is

$$H = \frac{\boldsymbol{k}^2}{2m} + \alpha(k_x\sigma_y - k_y\sigma_x) - \boldsymbol{B}\cdot\boldsymbol{\sigma}, \tag{7}$$

with m, $\boldsymbol{k}$, α, $\boldsymbol{B}$, and $\boldsymbol{\sigma}$ being the electron mass, electron wave number, Rashba parameter, magnetic field, and the Pauli matrix for real spins, respectively. Here, we consider the in-plane magnetic field since the out-plane field does not produce nonreciprocal charge transport. The band dispersion without magnetic field is schematically illustrated in Fig. 1(a). If the Rashba splitting $m\alpha^2$ is larger than T_0 or the superconducting gap, only the pairing in each spin-split band is relevant. Then, if both even-parity and odd-parity interactions exist, the parity of the superconducting order parameters is mixed.

To make the discussion simple, we fix the form of the interaction Hamiltonian in the band basis as [18]

$$H_{\rm int} = -\sum_{\boldsymbol{k}\boldsymbol{k}'\lambda\lambda'} t_{\boldsymbol{k}\lambda} t^*_{\boldsymbol{k}'\lambda'} \hat{g}_{\lambda\lambda'} \psi^\dagger_{\boldsymbol{k}\lambda} \psi^\dagger_{-\boldsymbol{k}\lambda} \psi_{-\boldsymbol{k}'\lambda'} \psi_{\boldsymbol{k}'\lambda'}, \tag{8}$$

where $\psi^\dagger_{\boldsymbol{k}\lambda}$ and $\psi_{\boldsymbol{k}\lambda}$ are the creation and annihilation operators with the band index $\lambda = \pm$, and $t_{\boldsymbol{k}\lambda} = \lambda i e^{i\phi_{\boldsymbol{k}}}$ with $\phi_{\boldsymbol{k}} = \arg(k_x + ik_y)$. We have assumed that the spin splitting due to

the Rashba interaction is much larger than the superconducting mean field temperature ($m\alpha^2 \gg T_0$) and, hence, the interband pairings are neglected.

We have also assumed the interactions in the spin basis which makes the matrix $\hat{g}$ independent on $\boldsymbol{k}$. The even-parity channel is the standard BCS-type onsite interaction

$$-V^{\mathrm{g}} \sum_{\boldsymbol{k}\boldsymbol{k}'} c^{\dagger}_{\boldsymbol{k}\uparrow} c^{\dagger}_{-\boldsymbol{k}\downarrow} c_{-\boldsymbol{k}'\downarrow} c_{\boldsymbol{k}'\uparrow}, \tag{9}$$

where $c^{\dagger}_{\boldsymbol{k}\sigma}$ and $c_{\boldsymbol{k}\sigma}$ are the creation and annihilation operators of the electron with momentum $\boldsymbol{k}$ and spin σ. The odd-parity channel is

$$-\sum_{\boldsymbol{k}\boldsymbol{k}'} V^{\mathrm{u}}_{ij}(\boldsymbol{k},\boldsymbol{k}')(i\sigma_i\sigma_2)_{\alpha\beta}(i\sigma_j\sigma_2)_{\gamma\delta} c^{\dagger}_{\boldsymbol{k}\alpha} c^{\dagger}_{-\boldsymbol{k}\beta} c_{-\boldsymbol{k}'\gamma} c_{\boldsymbol{k}'\delta}, \tag{10}$$

with $V^{\mathrm{u}}_{ij}(\boldsymbol{k},\boldsymbol{k}') = V^{\mathrm{u}} \hat{\gamma}_i(\boldsymbol{k}) \hat{\gamma}_j(\boldsymbol{k}')$ and $\hat{\boldsymbol{\gamma}}(\boldsymbol{k}) = \frac{1}{k}(-k_y, k_x)$. Then, the matrix $\hat{g}$ in Eq. (8) is

$$\hat{g} = \begin{pmatrix} g_1 & g_2 \\ g_2 & g_1 \end{pmatrix}, \tag{11}$$

with $g_1 = (V^{\mathrm{g}} + V^{\mathrm{u}})/4$ (> 0) and $g_2 = (V^{\mathrm{g}} - V^{\mathrm{u}})/4$.

In the following, we focus on two limiting cases. (1) $|V^{\mathrm{u}}| \ll |V^{\mathrm{g}}|$ (or, equivalently, $g_2 \approx g_1$) case. The singlet pairing is dominant and the triplet mixing is proportional to the parameter $r_{\mathrm{t}} = \frac{g_1 - g_2}{g_1}$, which we treat perturbatively. (2) $|V^{\mathrm{u}}| \gg |V^{\mathrm{g}}|$ (or, equivalently, $g_2 \approx -g_1$) case. In this case, the triplet pairing is dominant and the singlet mixing parameter is given by $r_{\mathrm{s}} = \frac{g_1 + g_2}{g_1}$.

In order to treat the parity mixing, the two-component GL theory has been employed. We assume that the Fermi energy E_{F} is on the conduction band ($E_{\mathrm{F}} > 0$) since the nonreciprocal paraconductivity vanishes for $E_{\mathrm{F}} < 0$ [18] in sharp contrast to that in the normal state [9]. The derivation of the GL free energy is shown in Ref. [18], and the result is

$$F = \int \frac{d^2\boldsymbol{q}}{(2\pi)^2} \sum_{\lambda\lambda'} \Delta^*_{\lambda}[(\hat{g}^{-1})_{\lambda\lambda'} + \delta_{\lambda\lambda'} N_{\lambda}(S_1 - L_{\lambda\boldsymbol{q}})]\Delta_{\lambda'}, \tag{12}$$

with the parameters

$$N_{\lambda} = \frac{m}{2\pi}\left(1 - \lambda \frac{\sqrt{m\alpha^2}}{\sqrt{E_{\mathrm{FR}}}}\right), \tag{13}$$

$$L_{\lambda\boldsymbol{q}} = K_{\lambda}\boldsymbol{q}^2 - \lambda R_{\lambda}(B_y q_x - B_x q_y), \tag{14}$$

$$K_- = K_+ = \frac{S_3 E_{\mathrm{FR}}}{8m}, \tag{15}$$

$$R_- = R_+ = \frac{S_3\sqrt{E_{\mathrm{FR}}}}{2\sqrt{m}}, \tag{16}$$

$$S_1 = \log\frac{2e^{\gamma_{\mathrm{E}}} E_{\mathrm{c}}}{\pi T}, \tag{17}$$

$$S_3 = \frac{7\zeta(3)}{4(\pi T)^2}. \tag{18}$$

We have defined $E_{\mathrm{FR}} = 2E_{\mathrm{F}} + m\alpha^2$, and γ_{E} is the Euler's constant, and E_{c} is the cutoff energy.

Then, the paraconductivity can be calculated as [10,17,18]

$$\boldsymbol{j} = -T\sum_{\boldsymbol{q}} C \left.\frac{\partial f(\boldsymbol{q} + 2e\boldsymbol{A})}{\partial \boldsymbol{A}}\right|_{\boldsymbol{A}=\boldsymbol{0}} \times \int_{-\infty}^{0} du\, \exp\left[-C\int_u^0 dt\, f(\boldsymbol{q} - 2e\boldsymbol{E}t)\right], \tag{19}$$

with $C = \frac{32T_0}{\pi\nu}$ and the density of states ν at the Fermi level. The function f is the eigenvalue of the matrix in Eq. (12) with a higher critical temperature. In the case of a single component GL free energy, f is defined as $F = \int \frac{d^2\boldsymbol{q}}{(2\pi)^2} f|\Delta|^2$. The paraconductivity is shown to be

$$j_x = \sigma_1 E_x + \sigma_2 E_x^2, \tag{20}$$

$$\sigma_1 = \frac{e^2}{16\epsilon}, \tag{21}$$

$$\sigma_2 = \frac{\pi e^3 B_y r_{\mathrm{t,s}}}{128\epsilon^2} \times \frac{N_- N_+ (K_- N_- - K_+ N_+)(K_- R_+ + K_+ R_-)}{S_1(T_0) T_0 (N_- + N_+)(K_- N_- + K_+ N_+)^2}, \tag{22}$$

in the lowest order of $r_{\mathrm{t,s}}$, and $\epsilon = \frac{T - T_0}{T_0}$ is the reduced temperature. It should be noted that the sign of the nonreciprocal current depends on the sign of $r_{\mathrm{t,s}}$, i.e., sign of V^{u} in the case of singlet dominant case and V^{g} in the case of triplet dominant case. The γ value [see Eq. (3)] is obtained by $W\gamma_{\mathrm{S}} = \sigma_2/(B\sigma_1^2)$ with W being the sample width [9,10,18]. The explicit form is

$$W\gamma_{\mathrm{S}} = \frac{\pi r_{\mathrm{t,s}} S_3 E_{\mathrm{F}} \alpha}{e S_1 T_0 E_{\mathrm{FR}}}. \tag{23}$$

For normal state, on the other hand, it can be shown that the nonreciprocal current exists in $E_{\mathrm{F}} < 0$ within the Boltzmann theory, where the γ value is given by $W\gamma_{\mathrm{N}} \sim \alpha/e(m\alpha^2 E_{\mathrm{FR}})^{3/2}$ [9]. In the case of $E_{\mathrm{F}} > 0$, the normal contribution is zero and there is only the paraconductivity contribution for the superconducting fluctuation regime. If we assume that the Rashba splitting is comparable to the Fermi energy in both cases, the ratio is $\gamma_{\mathrm{S}}(E_{\mathrm{F}} > 0)/\gamma_{\mathrm{N}}(E_{\mathrm{F}} < 0) \sim r_{\mathrm{t,s}}|E_{\mathrm{F}}|^3/(S_1 T_0^3)$.

We emphasize that the above nonreciprocity originates from the parity mixing [$r_{\mathrm{t,s}}$ in Eq. (23)]. In the next subsection, we will show another mechanism, which relies on the cubic term with respect to the momentum of the superconducting order parameter.

2. q-cubic term

Now, we consider the nonreciprocal paraconductivity in the Rashba superconductor without parity mixing. In contrast to the previous subsection, we consider the case only for the s-wave pairing. Although the expansion up to the second order of the momentum of the order parameter does not create finite nonreciprocal current, we have finite nonreciprocal current by considering the expansion up to the third order. The GL free energy for the s-wave order parameter can be obtained from the two-component GL free energy written with the band basis. If we diagonalize the two-component GL free energy in the band basis, the free energy for the s-wave order parameter is found to be a sum of the diagonal components.

We first define the three Fermi wave numbers and the density of states which correspond to (1) inner branch of the upper band, (2) inner branch of the lower band, and (3) outer branch:

$$k_{\mathrm{F1}} = -m\alpha + \sqrt{mE_{\mathrm{FR}}}, \tag{24}$$

$$k_{\mathrm{F2}} = m\alpha - \sqrt{mE_{\mathrm{FR}}}, \tag{25}$$

$$k_{\mathrm{F3}} = m\alpha + \sqrt{mE_{\mathrm{FR}}}, \tag{26}$$

$$\nu_1 = \frac{m}{2\pi}(1 - \alpha\sqrt{m/E_{\mathrm{FR}}}), \tag{27}$$

$$\nu_2 = \frac{m}{2\pi}(-1 + \alpha\sqrt{m/E_{\mathrm{FR}}}), \tag{28}$$

$$\nu_3 = \frac{m}{2\pi}(1 + \alpha\sqrt{m/E_{\mathrm{FR}}}). \tag{29}$$

The three wave vectors are graphically shown in Fig. 1(a). Then, we can derive the contribution from each branch separately, whose example is shown in Appendix A. To write the GL free energy in a simple form, we define the following functions:

$$f_A = \frac{E_{\mathrm{FR}}}{8m}\boldsymbol{q}^2 + \frac{3B_y}{32m\sqrt{mE_{\mathrm{FR}}}}\left(5 + \frac{3m\alpha}{-m\alpha + \sqrt{mE_{\mathrm{FR}}}}\right)q_x\boldsymbol{q}^2, \tag{30}$$

$$f_B = \frac{E_{\mathrm{FR}}}{8m}\boldsymbol{q}^2 + \frac{3B_y}{32m\sqrt{mE_{\mathrm{FR}}}}\left(-5 + \frac{3m\alpha}{m\alpha + \sqrt{mE_{\mathrm{FR}}}}\right)q_x\boldsymbol{q}^2, \tag{31}$$

where we have assumed $B_x = 0$ because it does not affect the conductivity along the x direction. In the case of $E_{\mathrm{F}} > 0$, the free energy is then

$$F = \int \frac{d^2\boldsymbol{q}}{(2\pi)^2}\left[\frac{1}{g} - (\nu_1 + \nu_3)S_1 + S_3(\nu_1 f_A + \nu_3 f_B)\right]|\Delta_{\boldsymbol{q}}|^2, \tag{32}$$

with g being the amplitude of the attractive interaction. Although the $\boldsymbol{q}$-linear term in general appears, it can be absorbed by a constant shift in $\boldsymbol{q}$ space and does not explicitly appear in the final results. The paraconductivity obtained from Eq. (19) is given by

$$j_x = \frac{e^2}{16\epsilon}E_x + \frac{3\pi e^3\alpha B_y}{512E_{\mathrm{FR}}^2 T_0\epsilon^2}E_x^2. \tag{33}$$

Correspondingly, the γ value is

$$W\gamma_{\mathrm{S}} = \frac{3\pi\alpha}{2eE_{\mathrm{FR}}^2 T_0}. \tag{34}$$

We also consider the case of $E_{\mathrm{F}} < 0$. The free energy is given by

$$F = \int \frac{d^2\boldsymbol{q}}{(2\pi)^2}\left[\frac{1}{g} - (\nu_2 + \nu_3)S_1 + S_3(\nu_2 f_A + \nu_3 f_B)\right]|\Delta_{\boldsymbol{q}}|^2. \tag{35}$$

Accordingly, we obtain

$$j_x = \frac{e^2}{16\epsilon}E_x + \frac{15\pi e^3 B_y}{1024m\alpha E_{\mathrm{FR}} T_0\epsilon^2}E_x^2, \tag{36}$$

and the γ value is

$$W\gamma_{\mathrm{S}} = \frac{15\pi}{4em\alpha E_{\mathrm{FR}} T_0}. \tag{37}$$

Thus, we have shown that the simple Rashba model (7) has the nonreciprocal current if we consider the GL free energy up to $O(\boldsymbol{q}^3)$. This mechanism is different from the previous subsection, where the singlet and triplet parity mixing is essential for the nonreciprocal current [18]. We note that the results for $E_{\mathrm{F}} > 0$ and $E_{\mathrm{F}} < 0$ do not connect continuously at $E_{\mathrm{F}} = 0$ since we have assumed that the Fermi energy is much larger than the superconducting transition temperature ($|E_{\mathrm{F}}| \gg T_0$).

Let us compare the nonreciprocal paraconductivities with and without parity mixing. The ratio between the γ value from the parity mixing mechanism (23) (denoted as $\gamma_{\mathrm{S}}^{\mathrm{pm}}$), and the γ value from the cubic term (37) (denoted as $\gamma_{\mathrm{S}}^{\mathrm{c}}$) is

$$\frac{\gamma_{\mathrm{S}}^{\mathrm{pm}}}{\gamma_{\mathrm{S}}^{\mathrm{c}}} \sim \frac{r_{\mathrm{t,s}}E_{\mathrm{F}}E_{\mathrm{FR}}}{S_1 T_0^2}. \tag{38}$$

If the even-parity interaction corresponds to the onsite interaction and the odd-parity interaction corresponds to the nearest-neighbor interaction, their amplitudes are roughly estimated as e^2/a_0 and e^2/a with a_0 and a being the Bohr radius and the lattice constant, respectively. Therefore, $r_{\mathrm{t,s}} \sim 0.1$ is reasonable value for the singlet dominant case, and Eq. (38) takes a large value. Hence, the nonreciprocity from the parity mixing is dominant. However, in the case of $E_{\mathrm{F}} < 0$, the nonreciprocal paraconductivity is from the cubic term mechanism because the parity mixing does not create nonreciprocity in that regime [18].

B. Surface state of topological insulator

1. *Parabolic dispersion*

We consider the nonreciprocal paraconductivity in the superconducting surface state of a topological insulator. The simplest Hamiltonian for the surface state is

$$H = v_{\mathrm{F}}(k_x\sigma_y - k_y\sigma_x) - \boldsymbol{B}\cdot\boldsymbol{\sigma}, \tag{39}$$

with v_{F} (>0) being the Fermi velocity and the magnetic field is applied along the in-plane direction. The dispersion relation is shown in Fig. 1(b). Since the in-plane magnetic field simply shifts the momentum and does not affect the transport, additional terms are necessary for the nonreciprocal current.

In this section, we include the term proportional to $\boldsymbol{k}^2$, whose Hamiltonian form is equivalent to Eq. (7), with α replaced with the Fermi velocity v_{F}. However, the first (parabolic) term here is much smaller than the second ($\boldsymbol{k}$-linear) term. Therefore, we will consider the asymptotic form for large m. Furthermore, we take into account only the inner branch of the Fermi surfaces. The eigenenergies are

$$\xi_{\boldsymbol{k}} = \frac{\boldsymbol{k}^2}{2m} - E_{\mathrm{F}} \pm \sqrt{(v_{\mathrm{F}}k_x - B_y)^2 + (v_{\mathrm{F}}k_y)^2}, \tag{40}$$

with the Fermi energy E_{F} included. We first assume that the Fermi energy is on the conduction band [plus sign in Eq. (40) and $E_{\mathrm{F}} > 0$]. We calculate the GL free energy and the detailed

derivation is shown in Appendix A. The result is

$$F = \int \frac{d^2\boldsymbol{q}}{(2\pi)^2}\left[\frac{1}{g} - \nu_1 S_1(T) + \nu_1 S_3(T)\left(\frac{(k_{\mathrm{F}1} + m v_{\mathrm{F}})^2}{8m^2}\boldsymbol{q}^2 + \frac{3(5k_{\mathrm{F}1} + 3m v_{\mathrm{F}})}{32mk_{\mathrm{F}1}(k_{\mathrm{F}1} + m v_{\mathrm{F}})} B_y q_x \boldsymbol{q}^2\right)\right]|\Delta_{\boldsymbol{q}}|^2. \tag{41}$$

We can also show that the free energy in the case where E_{F} is located on the valence band ($E_{\mathrm{F}} < 0$) is obtained by replacing v_{F} with $-v_{\mathrm{F}}$, B_y with $-B_y$, ν_1 with ν_2, and $k_{\mathrm{F}1}$ with $k_{\mathrm{F}2}$. It is noted that the cubic term with respect to the wave number vanishes for $m \to \infty$, which is consistent with the fact that the in-plane magnetic field simply shifts the momentum of the Cooper pairs without the parabolic term.

The paraconductivity up to $O(E_x^2 B_y)$ can be obtained by applying Eq. (19) as

$$j_x = \frac{e^2}{32\epsilon} E_x - \frac{3\pi e^3 m(5\sqrt{mE_{\mathrm{FR}}} - 2m v_{\mathrm{F}})B_y}{4096(mE_{\mathrm{FR}})^{3/2}(\sqrt{mE_{\mathrm{FR}}} - m v_{\mathrm{F}})T_0\epsilon^2} E_x^2. \tag{42}$$

The temperature dependence of the conductivity is the same as those of the transition-metal dichalcogenides and the Rashba superconductors [10,18]. We can also show that the case for $E_{\mathrm{F}} < 0$ has the same form, and the sign of the nonreciprocal current compared to the $E_{\mathrm{F}} > 0$ case is reversed.

The corresponding γ value is

$$W\gamma_{\mathrm{S}} = -\frac{3\pi m(5\sqrt{mE_{\mathrm{FR}}} - 2m v_{\mathrm{F}})}{4e(mE_{\mathrm{FR}})^{3/2}(\sqrt{mE_{\mathrm{FR}}} - m v_{\mathrm{F}})T_0}, \tag{43}$$

and for $m \to \infty$

$$W\gamma_{\mathrm{S}} \to -\frac{9\pi}{4em v_{\mathrm{F}} E_{\mathrm{F}} T_0}, \tag{44}$$

which is a leading contribution in the limit of a small parabolic term.

Now, we compare the γ value with that of the normal state. The normal-state conductivity is calculated by the Boltzmann equation with the relaxation time approximation [9]

$$\begin{aligned} j_x &= -\tau e^2 E_x \int \frac{d^2\boldsymbol{k}}{(2\pi)^2} v_{\boldsymbol{k}} \partial_{k_x} f_{\boldsymbol{k}} - \tau^2 e^3 E_x^2 \int \frac{d^2\boldsymbol{k}}{(2\pi)^2} v_{\boldsymbol{k}} \partial_{k_x}^2 f_{\boldsymbol{k}} \\ &= \tau e^2 E_x \int \frac{d^2\boldsymbol{k}}{(2\pi)^2} v_{\boldsymbol{k}}^2 \delta(\xi_{\boldsymbol{k}}) \\ &\quad - \tau^2 e^3 E_x^2 \int \frac{d^2\boldsymbol{k}}{(2\pi)^2} \partial_{k_x} v_{\boldsymbol{k}} v_{\boldsymbol{k}} \delta(\xi_{\boldsymbol{k}}), \end{aligned} \tag{45}$$

where $\xi_{\boldsymbol{k}}$ is the eigenenergy, $v_{\boldsymbol{k}} = \frac{\partial \xi_{\boldsymbol{k}}}{\partial k_x}$ is the group velocity, and τ is the relaxation time. The Fermi distribution function is also defined by $f_{\boldsymbol{k}} = 1/(e^{\beta\xi_{\boldsymbol{k}}} + 1)$. With use of this, we obtain the electronic current

$$j_x = \frac{e^2\tau\left(E_{\mathrm{FR}} - \sqrt{m v_{\mathrm{F}}^2 E_{\mathrm{FR}}}\right)}{4\pi} E_x - \mathrm{sgn}(E_{\mathrm{F}}) \frac{3e^3\tau^2 B_y}{16\pi\sqrt{mE_{\mathrm{FR}}}} E_x^2. \tag{46}$$

The γ value is

$$W\gamma_{\mathrm{N}} = -\mathrm{sgn}(E_{\mathrm{F}}) \frac{3\pi}{e\sqrt{mE_{\mathrm{FR}}}\left(E_{\mathrm{FR}} - \sqrt{m v_{\mathrm{F}}^2 E_{\mathrm{FR}}}\right)^2}, \tag{47}$$

and for $m \to \infty$

$$W\gamma_{\mathrm{N}} \to -\mathrm{sgn}(E_{\mathrm{F}}) \frac{3\pi}{em v_{\mathrm{F}} E_{\mathrm{F}}^2}. \tag{48}$$

Therefore, the ratio is

$$\frac{\gamma_{\mathrm{S}}}{\gamma_{\mathrm{N}}} \to \frac{3|E_{\mathrm{F}}|}{4T_0}, \tag{49}$$

which does not depend on m and v_{F}. The enhancement of the nonreciprocity by the factor of E_{F}/T_0 is expected in the superconducting fluctuation regime, although the power of enhancement is different from the TMD [10], in which $\gamma_{\mathrm{S}}/\gamma_{\mathrm{N}} \sim (E_{\mathrm{F}}/T_0)^3$. It should be noted that the direction of the nonreciprocal current is reversed between the conduction and valence bands in both of the paraconductivity and normal conductivity.

2. *Hexagonal warping*

The surface band of topological insulators such as Bi_2Te_3 or Bi_2Se_3 is hexagonally distorted because of the crystal symmetry [22]. We consider the effect of the hexagonal warping on the nonreciprocal paraconductivity. The Hamiltonian is

$$H = v_{\mathrm{F}}(k_x\sigma_y - k_y\sigma_x) + \frac{\sqrt{\lambda}}{2}(k_+^3 + k_-^3)\sigma_z - B_y\sigma_y, \tag{50}$$

with $k_\pm = k_x \pm ik_y$ and λ describes the strength of the hexagonal warping. The corresponding GL free energy can be obtained in a similar manner to the previous subsection. The free energy up to $O(\boldsymbol{q}^3 B_y \lambda)$ is

$$F = \int \frac{d^2\boldsymbol{q}}{(2\pi)^2}\left\{\frac{1}{g} - \nu S_1(T) + \nu S_3(T) \times \left[\left(\frac{v_{\mathrm{F}}^2}{8} + \frac{5\lambda k_{\mathrm{F}}^4}{16}\right)\boldsymbol{q}^2 + \frac{37k_{\mathrm{F}}^2\lambda}{8v_{\mathrm{F}}} B_y q_x \boldsymbol{q}^2\right]\right\}|\Delta_{\boldsymbol{q}}|^2, \tag{51}$$

with $v_{\mathrm{F}}k_{\mathrm{F}} = |E_{\mathrm{F}}|$ and the density of states ν at the Fermi level. The paraconductivity is obtained as

$$j_x = \frac{e^2}{32\epsilon} E_x - \frac{37\pi e^3 E_{\mathrm{F}}^2 \lambda B_y}{1024 v_{\mathrm{F}}^5 T_0 \epsilon^2} E_x^2. \tag{52}$$

Consequently, the γ value is

$$W\gamma_{\mathrm{S}} = -\frac{37\pi E_{\mathrm{F}}^2 \lambda}{e v_{\mathrm{F}}^5 T_0}. \tag{53}$$

We also calculate the normal-state current based on Eq. (45). We express $\boldsymbol{k}$ in the polar coordinate (k, θ), and solve $\xi_{\boldsymbol{k}} = 0$ up to $O(B_y\lambda)$ with fixed θ. Then, the integrals over k and θ can be carried out. The result is

$$j_x = \frac{\pi\tau e^2 |E_{\mathrm{F}}|\left(1 + E_{\mathrm{F}}^4\lambda/v_{\mathrm{F}}^6\right)}{4\pi^2} E_x - \frac{9\tau^2 e^3 |E_{\mathrm{F}}|^3 \lambda B_y}{2\pi v_{\mathrm{F}}^5} E_x^2. \tag{54}$$

The γ value is

$$W\gamma_{\mathrm{N}} = -\frac{72\pi |E_{\mathrm{F}}|\lambda}{e v_{\mathrm{F}}^5}. \tag{55}$$

Therefore, the ratio of the γ value of the paraconductivity and normal conductivity is

$$\frac{\gamma_S}{\gamma_N} = \frac{37|E_F|}{72T_0}, \tag{56}$$

which again does not depend on v_F and λ. The order of magnitude of the enhancement factor is the same as that for the parabolic dispersion case. We emphasize that the direction of the nonreciprocal current does not change between the conduction and valence bands in both of the paraconductivity and normal conductivity, which is clearly different from the nonreciprocal current originates from the parabolic term in the previous subsection.

C. Transition-metal dichalcogenides

The nonreciprocal paraconductivity in two-dimensional TMD has been investigated both theoretically and experimentally [10]. Here, we summarize these results. The normal-state Hamiltonian around the K and K' valleys is

$$H_{k\sigma\tau} = \frac{\boldsymbol{k}^2}{2m} + \tau_z \lambda k_x \left(k_x^2 - 3k_y^3\right) - \Delta_Z \sigma_z - \Delta_{SO}\sigma_z\tau_z, \tag{57}$$

with $\boldsymbol{k}$, m, λ, $\Delta_Z = B_z$, and Δ_{SO} being the electron wave number, mass, amplitude for the trigonal warping, Zeeman splitting, and spin-orbit splitting, respectively. The x axis is taken along a "zigzag" chain in the honeycomb lattice, and the y axis is along "armchair" direction. The out-of-plane magnetic field is necessary for the nonreciprocal current. The symbols σ_z and τ_z represent the Pauli matrices for the spin $(\uparrow, \downarrow)$ and valley degrees of freedom (K, K'), respectively, and take the values ± 1. The dispersion relation is schematically shown in Fig. 1(c). In contrast to the previous Rashba system and TI surface, the nonreciprocal response is present even for the out-plane magnetic field due to the trigonal warping parameter λ. While this study is designed for MoS_2, a similar behavior is also expected for the other TMDs which have trigonal distortion.

The GL free energy for the superconducting state can be derived based on Eq. (57). The free energy up to $O(\Delta_Z \lambda \boldsymbol{q}^3)$ is

$$F = \int \frac{d^2\boldsymbol{q}}{(2\pi)^2} \Psi_{\boldsymbol{q}}^* \left[a + \frac{\boldsymbol{q}^2}{4m} + \Lambda B_z \left(q_x^3 - 3q_x q_y^2\right)\right] \Psi_{\boldsymbol{q}}, \tag{58}$$

with $\Lambda = \frac{93\zeta(5)}{14\zeta(3)} \frac{\Delta_{SO}\lambda}{(\pi T_0)^2}$. The effect of nonmagnetic impurities can also be considered, whose derivation is summarized in Appendix B. By applying Eq. (19) for Eq. (58), the current up to the second order of electric field is obtained as

$$\boldsymbol{j} = \frac{e^2}{16\epsilon}\boldsymbol{E} - \frac{\pi e^3 m \Lambda B}{64 T_0 \epsilon^2} \boldsymbol{F}(\boldsymbol{E}), \tag{59}$$

with $\boldsymbol{F}(\boldsymbol{E}) = (E_x^2 - E_y^2, -2E_x E_y)$, which is consistent with the crystal symmetry of the transition-metal dichalcogenides. The γ value is

$$W\gamma_S = \frac{4\pi m \Lambda}{eT_0}. \tag{60}$$

On the other hand, the γ value for the normal state can be obtained by the Boltzmann equation [9], whose typical value is calculated as $W\gamma_N \sim m\Delta_{SO}\lambda/(eE_F^3)$ [10]. The ratio between the superconducting fluctuation and normal regimes is found to be $\gamma_S/\gamma_N \sim (E_F/T_0)^3$, which is quite large. While the focus of this paper is on the region at small magnetic fields, we can also consider the high magnetic field region by including the Landau level, which is discussed in Appendix C.

III. VORTEX IN NONCENTROSYMMETRIC SUPERCONDUCTORS

When the superconducting gap function is sufficiently developed below T_0, the phase of the order parameter forms the vortices whose dynamics governs electronic transport properties. In this section, we begin with the phenomenological discussion for the nonreciprocity entering through the renormalization of the superfluid density, which captures the essence of the nonreciprocal vortex dynamics. In Sec. III C, we also consider the the ratchet potential effect for the vortices, which is necessarily present for noncentrosymmetric superconductors with trigonal symmetry and disorder effects.

A. Renormalization of superfluid density

1. Modified KT transition point for a system with in-plane magnetic field

Let us first consider the system with the in-plane magnetic field. In this case, the vortices and antivortices are generated thermally above the KT transition temperature. We take a Rashba ($E_F < 0$) or TI-based system with in-plane magnetic field, whose free-energy density is in general given by

$$f = \tfrac{1}{2}\rho_s \boldsymbol{v}_s^2 + \Lambda' B_y \rho_s v_{sx} \boldsymbol{v}_s^2, \tag{61}$$

which is phenomenologically introduced by utilizing the replacement $\boldsymbol{q} \to m^*\boldsymbol{v}_s$ in the GL theory. Here, $\rho_s = m^* n_s$ and $\boldsymbol{v}_s$ are superfluid mass density and velocity, respectively. Let us relate the phenomenological parameters m^* and Λ' to those in the original electronic Hamiltonians discussed in Sec. II. For Rashba superconductor, the specific forms of the parameters are given from Eq. (32) as

$$m^* \sim m, \quad \Lambda' \sim -\frac{\sqrt{m}}{|E_F|^{3/2}}, \tag{62}$$

where we have assumed that the energy scales for the Fermi energy and Rashba energy splitting are similar: $|E_F| \sim m\alpha^2$. The expressions for the TI surface with parabolic dispersion are obtained from Eq. (41) as

$$m^* \sim \frac{|E_F|}{v_F^2}, \quad \Lambda' \sim \frac{\mathrm{sgn}\, E_F}{m v_F^3}. \tag{63}$$

We have taken $m \to \infty$ in the final expressions. When we consider the contribution from the hexagonal warping in Eq. (51) for the TI surface, the parameters are

$$m^* \sim \frac{|E_F|}{v_F^2}, \quad \Lambda' \sim \frac{\lambda |E_F|^3}{v_F^7}, \tag{64}$$

where we have expanded the expressions with respect to the warping parameter λ.

We use a mean field approach for analysis, in which the terms higher than second order are approximated into quadratic one. Under the externally induced current, the superfluid acquires the uniform velocity component $\boldsymbol{v}_{unif}$. Hence, we can replace one of $\boldsymbol{v}_s$ by $\boldsymbol{v}_{unif}$ in the third-order term and obtain the

free-energy density

$$f \simeq \frac{1}{2}\sum_{\mu\nu}\tilde{\rho}_{s,\mu\nu}v_{s\mu}v_{s\nu}, \tag{65}$$

$$\tilde{\rho}_s = \rho_s\begin{pmatrix} 1+6\Lambda' B_y v_{\mathrm{unif},x} & 2\Lambda' B_y v_{\mathrm{unif},y} \\ 2\Lambda' B_y v_{\mathrm{unif},y} & 1+2\Lambda' B_y v_{\mathrm{unif},x}\end{pmatrix}. \tag{66}$$

Thus, the uniform current renormalizes the superfluid density due to the presence of the $\boldsymbol{v}$-cubic term. If we choose $\boldsymbol{v}_{\mathrm{unif}} = v_{s0}\hat{\boldsymbol{x}}$, the free energy has the following form:

$$f \simeq \tfrac{1}{2}\rho_s(1+4\Lambda' B_y v_{s0})\left(v_{sx}^2+v_{sy}^2\right)+\rho_s\Lambda' B_y v_{s0}\left(v_{sx}^2-v_{sy}^2\right). \tag{67}$$

The first term here renormalizes the superfluid density isotropically:

$$\tilde{n}_s = n_s(1+4\Lambda' B_y v_{s0}). \tag{68}$$

The second term in Eq. (67) is the anisotropic renormalization, which will be discussed in detail in the next subsections. In the following, we follow the procedure given in Ref. [11] to calculate transport coefficients.

Let us consider the force between the thermally generated vortex and antivortex. This can be interpreted as the Magnus force acting on one vortex which is located in a nearly uniform current made by the other vortex. At KT transition point, this force is balanced by an entropic force proportional to temperature, which leads to the force balance relation for two vortices separated by the sufficiently large distance r [11,23]:

$$e^*\tilde{n}_s\frac{1}{m^* r}\times\Phi_0 = \frac{4\tilde{T}_{\mathrm{KT}}}{r}, \tag{69}$$

where $\Phi_0 = 2\pi/|e^*|$ is the magnetic flux quantum and $e^* = 2e$. Thus, the important consequence of the isotropically renormalized superfluid density is the modification of the KT transition temperature $\tilde{T}_{\mathrm{KT}}$ through $\tilde{n}_s$ in Eq. (68), which has different values depending on the direction of the uniform current.

Through the change in T_{KT}, the correlation length ξ_+, which is exponentially diverging near T_{KT}, and the density of unpaired vortices n_{v} are also affected by $\boldsymbol{v}_{\mathrm{unif}}$. These physical quantities are given near T_{KT} by [11,24]

$$\xi_+ = b^{-1/2}\xi_c\exp\left(\sqrt{b\frac{T_0-\tilde{T}_{\mathrm{KT}}}{T-\tilde{T}_{\mathrm{KT}}}}\right), \tag{70}$$

$$n_{\mathrm{v}} = (2\pi C_1\xi_+^2)^{-1}, \tag{71}$$

where b, C_1 are order of unity constants, and ξ_c is the GL coherence length evaluated at $T = T_{\mathrm{KT}}$. The mean field transition temperature is written as T_0. The value of n_{v} goes to zero at $\tilde{T}_{\mathrm{KT}}$ with only bounded vortices left. Since the correlation length is dependent of the KT transition temperature, this indicates that the number of vortices is different depending on the direction of the uniform current.

Now, we consider the electric field caused by the vortex dynamics [11]. With a uniform current, the thermally generated vortices feel a Magnus force and move with the velocity $\pm\boldsymbol{v}_{\mathrm{L}}$ perpendicular to $\boldsymbol{v}_{\mathrm{unif}}$. To convert a hydrodynamic effect to electric one, we use the Josephson relation $\Delta V = (1/e^*)d\Delta\theta/dt$ where ΔV and $\Delta\theta$ are voltage drop and phase difference between the two ends of the sample, respectively. The vortices with the number $n_{\mathrm{v}}L_x v_{\mathrm{L}}$ (L_x is the sample width along x direction) cross the sample edges per unit time, leading to the phase slip $d\Delta\theta/dt = 2\pi n_{\mathrm{v}}L_x v_{\mathrm{L}}$. The electric field $E_x = \Delta V/L_x$ is then given by

$$E_x = \frac{(2\pi)^2 n_{\mathrm{v}}}{|e^*|^2\eta}j_{\mathrm{unif},x}, \tag{72}$$

where we have used the force balance relation $j_{\mathrm{unif},x}\Phi_0 = \eta v_{\mathrm{L}}$ between Magnus force and friction force. The uniform electric current has been defined by $\boldsymbol{j}_{\mathrm{unif}} = -\partial f/\partial\boldsymbol{A} = \frac{e^*}{m^*}\partial f/\partial\boldsymbol{v}_{\mathrm{unif}} = e^* n_s\boldsymbol{v}_{\mathrm{unif}} + O(\boldsymbol{v}_{\mathrm{unif}}^2)$, whose higher-order terms do not modify the conclusion for the γ value. The friction coefficient is given by $\eta = \eta_0(1+d_0\Lambda' B_y v_{s0})$ with d_0 being a constant and $\eta_0 \simeq \pi\sigma_n/(e^*)^2\xi_c^2$. This modification enters due to the anisotropic renormalization of superfluid density. The derivation is given in Secs. III A 2 and III B in detail, and here we just employ the final results. Substituting these expressions, we obtain the resistivity

$$\rho = \frac{2(1-d_0\Lambda' B_y v_{s0})}{C_1\sigma_n}\left(\frac{\xi_c}{\xi_+}\right)^2. \tag{73}$$

Thus, there are two kinds of the sources for nonreciprocal response: one is from the modified KT transition temperature and the other from the modified friction coefficient. By extrapolating the above expression to $T \to T_0$, the exponential temperature dependence in the correlation length is not effective. In this case, with the transport coefficients defined in $E_x = \rho_1 j_{\mathrm{unif},x} + \rho_2 j_{\mathrm{unif},x}^2$, we obtain the explicit expressions

$$\rho_1 = \frac{2b}{C_1\sigma_n}, \tag{74}$$

$$\rho_2(T) = -\frac{d_0\Lambda' B_y}{e^* n_s(T)}\rho_1. \tag{75}$$

We then find that the γ value, which is given by $\gamma_{\mathrm{S}}^{\mathrm{v}} = -\rho_2/\rho_1 B_y W$, is proportional to $(T_0-T)^{-1}$, where we have used the temperature dependence of the superfluid density as $n_s(T) \propto T_0 - T$.

We now switch our discussion to the lower temperatures near the KT transition. We write the KT transition temperature as $\tilde{T}_{\mathrm{KT}} = T_{\mathrm{KT}} + \delta T_{\mathrm{KT}}$ with the unrenormalized transition temperature T_{KT}, and expand the expression with respect to δT_{KT}. We assume $T_0 - T_{\mathrm{KT}} \gg \delta T_{\mathrm{KT}}$ and then the transport coefficients are given for the temperature range $T - T_{\mathrm{KT}} \gg \delta T_{\mathrm{KT}}$ by

$$\rho_1(T) = \frac{2b}{C_1\sigma_n}\exp\left(-2\sqrt{b\frac{T_0-T_{\mathrm{KT}}}{T-T_{\mathrm{KT}}}}\right), \tag{76}$$

$$\rho_2(T) = -\frac{2\pi\Lambda' B_y\sqrt{b(T_0-T_{\mathrm{KT}})}}{m^* e^*(T-T_{\mathrm{KT}})^{3/2}}\rho_1(T), \tag{77}$$

where we have kept the leading-order contribution remaining for $T \to T_{\mathrm{KT}}$. While both ρ_1 and ρ_2 exponentially goes to zero toward T_{KT}, the γ value is proportional to $(T-T_{\mathrm{KT}})^{-3/2}$. Thus, a large nonreciprocal signal is expected near the KT transition point.

Below $T_{\rm KT}$, the linear response vanishes due to bounded vortices, and instead the third-order term characterizes the current-voltage relation. The nonreciprocal response should then be reflected in the fourth-order term. Hence, the I-V relation has the form $V = a_3 I^3 + a_4 I^4$ with $a_4 = a_4' B$ near $T_{\rm KT}$. The higher-order terms become more relevant at lower temperatures.

2. *Extended Bardeen-Stephen approach for a system with out-plane magnetic field*

While the vortices in a system with in-plane magnetic field are created by the thermal fluctuation, the out-plane magnetic field creates the vortices having the same vorticity, which is a qualitatively different situation from the in-plane case. We here extend the Bardeen-Stephen theory [25,26] for flux-flow conductivity to nonlinear response regime. We take the MoS_2-based system where the magnetic field is applied along out-plane direction. The nonreciprocity for this system is considered as an effective renormalization of the superfluid density. To see this, we begin with the free-energy density for a superfluid

$$f = \tfrac{1}{2}\rho_s \boldsymbol{v}_s^2 + \Lambda' B_z \rho_s v_{sx}\left(v_{sx}^2 - 3v_{sy}^2\right). \tag{78}$$

By comparing this expression with Eq. (58), we find the relations $m^* = 2m$ and $\Lambda' \sim m^2\Lambda$. We choose the uniform current flowing along x direction: $\boldsymbol{v}_{\rm unif} = v_{s0}\hat{\boldsymbol{x}}$. The free energy then becomes

$$f = \tfrac{1}{2}\left(\tilde{\rho}_{s,xx} v_{sx}^2 + \tilde{\rho}_{s,yy} v_{sy}^2\right), \tag{79}$$

$$\tilde{\rho}_{s,xx} = \rho_s(1 + 6\Lambda' B_z v_{s0}), \tag{80}$$

$$\tilde{\rho}_{s,yy} = \rho_s(1 - 6\Lambda' B_z v_{s0}), \tag{81}$$

within the "mean field" approximation explained above. Here, only the anisotropic renormalization occurs.

Using the velocity potential, the superfluid velocity can be written as $\boldsymbol{v}_s = \frac{1}{m^*}\nabla\theta$. Let us first consider the isolated superconducting vortex induced by the out-plane external magnetic field. The vortex velocity for isotropic system is given by $\theta = \phi = \tan^{-1}(y/x)$ with the polar coordinate $\boldsymbol{r} = (r, \phi)$, which satisfies the equation $\nabla^2\theta = 0$ obtained from a variational principle. We can make Eq. (79) isotropic by the scaling $x' = x\sqrt{\rho_s/\tilde{\rho}_{s,xx}}$ and $y' = y\sqrt{\rho_s/\tilde{\rho}_{s,yy}}$. In this case, the velocity potential is given by $\theta = \tan^{-1}(y'/x')$. Keeping the first-order contribution with respect to Λ', we get

$$\theta(\phi) = \phi + 3\Lambda' B_z v_{s0} \sin 2\phi. \tag{82}$$

In order to calculate the spatial distribution of electric field, we employ the London equation outside the normal core accounting for zero resistivity: $\boldsymbol{E} = \Lambda \partial_t \boldsymbol{j}_s$ where $\Lambda^{-1} = n_s(e^*)^2/m^*$ [25,26]. For a moving vortex with the velocity $\boldsymbol{v}_{\rm L}$, the spatial coordinate is replaced as $\boldsymbol{r} \to \boldsymbol{r} - \boldsymbol{v}_{\rm L}t$ and we can replace the time derivative as $\partial_t \to -\boldsymbol{v}_{\rm L}\cdot\nabla$. With a uniform current along x direction, the "Lorentz" force acting on the vortex is along y direction, so we choose $\boldsymbol{v}_{\rm L} = v_{\rm L}\hat{\boldsymbol{y}}$. (Since the magnetic penetration depth is very long for atomically thin two-dimensional superconductors, the force should originate from fluid-mechanical Magnus force [27], although the main conclusion in the following is not altered.) Substituting $\boldsymbol{j}_s = e^* n_s \boldsymbol{v}_s$ into the London equation, we can calculate the electric field in the superconducting region, where r is larger than the coherence length ξ, as

$$\begin{aligned}\boldsymbol{E}(r > \xi) = {}& \frac{v_{\rm L}}{e^* r^2}\cos\phi(1 + 6\Lambda' B_z v_{s0}\cos 2\phi)\boldsymbol{e}_r \\ & + \frac{v_{\rm L}}{e^* r^2}\sin\phi[1 + 6\Lambda' B_z v_{s0}(2 + 3\cos 2\phi)]\boldsymbol{e}_\phi.\end{aligned} \tag{83}$$

For the inside of the normal core ($r < \xi$), the electric field $\boldsymbol{E} = -\nabla\varphi$ is determined from the Poisson equation $\nabla^2\varphi = 0$ due to a charge neutrality. We assume that the boundary between superconducting and normal regions is circular at $r = \xi$ and is connected discontinuously. With this geometry, only the $\boldsymbol{e}_\phi$ component of $\boldsymbol{E}$ matters for the boundary condition. We expand the scalar potential as $\varphi = \sum_m C_m (re^{i\phi})^m$ and the boundary condition gives

$$\begin{aligned}\varphi(r < \xi) = {}& -\frac{v_{\rm L}}{e^*\xi^2}(1 + 3\Lambda' B_z v_{s0}) r\cos\phi \\ & - \frac{3 v_{\rm L}\Lambda' B_z v_{s0}}{e^*\xi^4} r^3 \cos 3\phi.\end{aligned} \tag{84}$$

The energy dissipation rate is then calculated as

$$W(r < \xi) = \sigma_n \boldsymbol{E}^2 = \frac{\sigma_n}{(e^*)^2\xi^4}(1 + 6\Lambda' B_z v_{s0}) v_{\rm L}^2, \tag{85}$$

where σ_n is a normal conductivity. We note that this expression does not depend on the spatial coordinate $\boldsymbol{r}$ in the leading order. Equation (85) is identified as the energy dissipation rate per unit volume in the form $\eta v_{\rm L}^2/\pi\xi^2$ originating from the friction force for the vortex flow. We thus arrive at an important conclusion that the effect of the cubic term in free energy is reflected in the change of the friction coefficient η.

The "Lorentz" force is balanced by the friction force as $(\boldsymbol{j}_{\rm unif} \times \boldsymbol{\Phi}_0)_y = \eta v_{\rm L}$ where $\eta = \eta_0(1 + 6\Lambda' B_z v_{s0})$ with $\eta_0 = \pi\sigma_n/(e^*)^2\xi^2$ and we have defined $\boldsymbol{\Phi}_0 = \Phi_0\hat{\boldsymbol{z}}$. We use the expressions for the uniform current $\boldsymbol{j}_{\rm unif} = e^* n_s \boldsymbol{v}_{\rm unif}$ and the "Faraday's law" $\boldsymbol{E}_0 = \boldsymbol{B} \times \boldsymbol{v}_{\rm L}$ for the uniform electric field generated from the flux flow. (Since the magnetic field $\boldsymbol{B}$ is not time dependent in the system with infinite magnetic penetration depth, this "Faraday's law" does not derive from an electromagnetic origin but from the Josephson relation as in the previous subsection.) We then obtain $E_{0x} = \rho_1 j_{{\rm unif},x} + \rho_2 j_{{\rm unif},x}^2$ where

$$\rho_1 = \frac{B_z\Phi_0}{\eta_0}, \tag{86}$$

$$\rho_2 = -\frac{6\Lambda' B_z^2\Phi_0}{e^* n_s \eta_0}. \tag{87}$$

The γ value from the vortex dynamics is given by

$$\gamma_{\rm S}^{\rm v} = -\frac{\rho_2}{\rho_1 B_z W} = \frac{6\Lambda'}{e^* n_s W}, \tag{88}$$

which is not dependent on the normal conductivity. Rewriting the coefficient Λ' in terms of the quantities in Sec. II C, we can estimate the ratio between $\gamma_{\rm S}^{\rm v}$ from vortex motion and $\gamma_{\rm S}^{\rm f}$ from

superconducting fluctuation as

$$\frac{\gamma_{\rm S}^{\rm v}}{\gamma_{\rm S}^{\rm f}} \sim \frac{mT_0}{n_s}. \tag{89}$$

Using the relations $2n_s/n_e \simeq (T_0 - T)/T_0$ and the normal electron density $n_e = k_{\rm F}^2/2\pi$, we finally obtain

$$\frac{\gamma_{\rm S}^{\rm v}}{\gamma_{\rm S}^{\rm f}} \sim \frac{T_0^2}{E_{\rm F}(T_0 - T)} \xrightarrow{T\to 0} \frac{T_0}{E_{\rm F}}. \tag{90}$$

It is characteristic that the γ value from vortex dynamics is enhanced near the transition temperature and has a smaller value with the factor $T_0/E_{\rm F}$ compared to $\gamma_{\rm S}^{\rm f}$ at low temperatures. The same conclusion will be obtained from the time-dependent Ginzburg-Landau (TDGL) approach as described in Sec. III B in detail, and hence the above approach can be justified.

B. TDGL approach

1. Formulation

The vortex dynamics induced by the out-plane magnetic field can be described by the TDGL theory, which takes account of a purely dissipative dynamics. This approach is successfully applied to the flux-flow conductivities [28,29]. While this theory is less intuitive than the above extended Bardeen-Stephen theory, the TDGL approach gives a foundation for its interpretation. Here, we formulate the theory by including the cubic term in $\boldsymbol{q}$ responsible for a nonreciprocal vortex dynamics. We begin with the TDGL equation and free energy

$$\Gamma(\partial_t + 2ie\varphi)\Delta = -\frac{\delta F}{\delta \Delta^*}, \tag{91}$$

$$F_s = \int d^2\boldsymbol{r}\, \Delta^* \left[\alpha + \frac{\beta}{2}|\Delta|^2 + \gamma \boldsymbol{P}^2 + K\left(P_x^3 - 3\overline{P_x P_y^2}\right)\right]\Delta + \frac{1}{2\mu_0}\int d^2\boldsymbol{r}\, \boldsymbol{B}^2, \tag{92}$$

where $\boldsymbol{P} = -i\boldsymbol{\nabla} - 2e\boldsymbol{A}$. The gap parameter is related to the wave function by $\Psi = \sqrt{\frac{7\zeta(3)n_e}{2\pi^2 T_0^2}}\,\Delta$ with the electron number n_e. There are also the relations $K \propto \Lambda B_z$ and $\alpha \propto (T_0 - T)$. Note that the coefficient γ in Eq. (92) is different from the γ value for nonreciprocal transport which is denoted as $\gamma_{\rm S}$. The total GL free energy is given by $F = F_s + F_n$ with F_n being a normal part. We have defined the symmetrization by

$$\overline{ABC} = \frac{1}{3!}(ABC + BCA + CAB + ACB + BAC + CBA), \tag{93}$$

to make the free energy real. The supercurrent density is given by $\delta F/\delta \boldsymbol{A} = 0$ as

$$j_{sx} = 2e\gamma(\Delta^* P_x \Delta + P_x^\dagger \Delta^* \Delta) + 2eK\left(\Delta^* P_x^2 \Delta + P_x^\dagger \Delta^* P_x \Delta + P_x^{\dagger 2}\Delta^*\Delta - \Delta^* P_y^2 \Delta - P_y^\dagger \Delta^* P_y \Delta - P_y^{\dagger 2}\Delta^*\Delta\right), \tag{94}$$

$$j_{sy} = 2e\gamma(\Delta^* P_y \Delta + P_y^\dagger \Delta^* \Delta) - 2eK(\Delta^* P_x P_y \Delta + \Delta^* P_y P_x \Delta + P_x^\dagger \Delta^* P_y \Delta + P_y^\dagger \Delta^* P_x \Delta + P_x^\dagger P_y^\dagger \Delta^*\Delta + P_y^\dagger P_x^\dagger \Delta^*\Delta). \tag{95}$$

The total current is given by $\boldsymbol{j} = \boldsymbol{j}_n + \boldsymbol{j}_s$ with the normal current $\boldsymbol{j}_n = \sigma_n \boldsymbol{E}$. We can also show the relations

$$\frac{\delta F}{\delta \Delta^*} = \left[\alpha + \beta|\Delta|^2 + \gamma \boldsymbol{P}^2 + K\left(P_x^3 - 3\overline{P_x P_y^2}\right)\right]\Delta \tag{96}$$

and

$$i\left(\Delta\frac{\delta F}{\delta \Delta} - \Delta^*\frac{\delta F}{\delta \Delta^*}\right) = -\frac{1}{2e}\boldsymbol{\nabla}\cdot\boldsymbol{j}_s. \tag{97}$$

The above expressions can be used for arbitrary strength of the magnetic field.

In the following, we concentrate on the two-dimensional superconductor where the magnetic penetration depth is typically longer than the sample size [30]. In this case, the magnetic effects can be neglected and only the electric and fluid mechanical effects are considered in the GL analysis. Such condition can be set by choosing $\boldsymbol{A} = \boldsymbol{0}$.

With a slightly shifted center as $\boldsymbol{r} \to \boldsymbol{r} + \boldsymbol{d}$, we have the relation

$$\delta F = \int d^2\boldsymbol{r}\left[\frac{\delta F}{\delta \Delta}(\boldsymbol{d}\cdot\boldsymbol{\nabla})\Delta + \text{c.c.}\right], \tag{98}$$

which defines a friction force acting on superconductor. This force is balanced by an external force to result in a stationary motion of the vortex. The force balance equation for an isolated single vortex is given by

$$\boldsymbol{j}_{\rm unif} \times \boldsymbol{\Phi}_0 = -\Gamma \int d^2\boldsymbol{r}[(\partial_t - 2ie\varphi)\Delta^*\boldsymbol{\nabla}\Delta + \text{c.c.}]. \tag{99}$$

The transport current from an external source is written as $\boldsymbol{j}_{\rm unif}$. The term on the left-hand side is the external force acting on the fluxoid, which is in general composed of the sum of Lorentz and Magnus forces [31]. In the current situation, only the Magnus force contributes [27] since the London magnetic penetration depth is taken as infinity.

We also need the equation for the scalar potential, for which the equation of continuity $\boldsymbol{\nabla}\cdot\boldsymbol{j} = 0$ is used. The explicit form is given by

$$\left(\frac{\sigma_n}{2e}\boldsymbol{\nabla}^2 - 4e\Gamma|\Delta|^2\right)\varphi = i\Gamma(\Delta\partial_t\Delta^* - \Delta^*\partial_t\Delta), \tag{100}$$

where we have used $\boldsymbol{E} = -\boldsymbol{\nabla}\varphi$.

For a moving vortex, the spatial coordinate can be written in the laboratory frame by the replacement $\boldsymbol{r} \to \boldsymbol{r} - \boldsymbol{v}_{\rm L}t$ with a boost velocity $\boldsymbol{v}_{\rm L}$ for the vortex. Correspondingly, we replace the time derivative as $\partial_t \to -\boldsymbol{v}_{\rm L}\cdot\boldsymbol{\nabla}$ and rewrite the equations with dimensionless quantities as

$$v\left(\hat{\boldsymbol{v}}_{\rm L}\cdot\tilde{\boldsymbol{\nabla}} - \frac{i}{2}\tilde{\varphi}\right)\psi = \left[-1 + |\psi|^2 - \tilde{\boldsymbol{\nabla}}^2 + ik\left(\tilde{\partial}_x^3 - 3\tilde{\partial}_x\tilde{\partial}_y^2\right)\right]\psi, \tag{101}$$

$$\left(\frac{1}{u}\tilde{\boldsymbol{\nabla}}^2 - |\psi|^2\right)\tilde{\varphi} = -i\hat{\boldsymbol{v}}_{\rm L}\cdot(\psi\tilde{\boldsymbol{\nabla}}\psi^* - \psi^*\tilde{\boldsymbol{\nabla}}\psi), \tag{102}$$

$$v = \frac{\Gamma v_{\rm L}}{|\alpha|\xi}, \quad k = \frac{K}{|\alpha|\xi^3}, \quad \psi = \frac{\Delta}{|\Delta_\infty|}, \quad \tilde{\varphi} = \frac{\varphi}{v_{\rm L}/4e\xi}, \tag{103}$$

where $|\Delta_\infty| = \sqrt{|\alpha|/\beta}$ is the gap function for a uniform bulk and $\xi = \sqrt{\gamma/|\alpha|}$ is the coherence length. We have also defined the unit vector $\hat{\boldsymbol{v}}_{\rm L} = \boldsymbol{v}_{\rm L}/v_{\rm L}$ and the dimensionless derivative $\tilde{\boldsymbol{\nabla}} = \xi\boldsymbol{\nabla}$. In the equation for the scalar potential, we have introduced the temperature-independent parameter $u = \xi^2/\ell_E^2$, where the length ℓ_E is the electric-field penetration depth given by

$$\ell_E = \sqrt{\frac{\sigma_n}{8e^2\Gamma|\Delta_\infty|^2}}. \tag{104}$$

For an ordinary metal, the parameter u is an order of unity constant [29].

When we use the relation $\Gamma = \pi\nu\hbar/8k_{\rm B}T_0$ with the density of states $\nu = m/2\pi\hbar^2$ for a two-dimensional electron gas, where we have restored $\hbar$ and $k_{\rm B}$, the parameter can be written as

$$u = \frac{\pi}{3}\frac{e^2/h}{\sigma_n}\frac{E_{\rm F}}{k_{\rm B}T_0}, \tag{105}$$

where $h/e^2 = 25813\,[\Omega]$ is the von Klitzing constant. For usual BCS superconductors, the ratio between e^2/h and the normal conductivity σ_n is comparable to $k_BT_0/E_{\rm F}$. For example, in the monolayer MoS_2 [10], we have $1/\sigma_n = 140\ (\Omega)$, $T_0 = 8.8$ (K), $E_{\rm F} = 150$ (meV), and obtain $u \simeq 1.2$.

The energy dissipation is also derived from the time derivative of free energy

$$\partial_t F_s = \int d^2\boldsymbol{r}[-2\Gamma|(\partial_t + 2ie\varphi)\Delta|^2 + \varphi\boldsymbol{\nabla}\cdot\boldsymbol{j}_s]. \tag{106}$$

Using the electromagnetic energy conservation law $\partial_t F_n = -\int d^2\boldsymbol{r}\,\boldsymbol{j}\cdot\boldsymbol{E}$ derived from the Maxwell equation, we obtain the equation of continuity for the energy density:

$$\partial_t F + \int d^2\boldsymbol{r}\,\boldsymbol{\nabla}\cdot\boldsymbol{j}_F = -\int d^2\boldsymbol{r}\,w, \tag{107}$$

$$\boldsymbol{j}_F = -\varphi\boldsymbol{j}_s, \tag{108}$$

$$w = 2\Gamma|(\partial_t + 2ie\varphi)\Delta|^2 + \sigma_n\boldsymbol{E}^2, \tag{109}$$

where $\boldsymbol{j}_F(\boldsymbol{r},t)$ is an energy current density and $w(\boldsymbol{r},t)$ is a dissipation rate. Thus, we have two kinds of the dissipation terms originating from Γ and σ_n.

2. *Perturbative analysis*

Let us now analyze the differential equation perturbatively with respect to K and $v_{\rm L}$. We expand the physical quantity A in general as

$$A = A_0 + kA_k + vA_v + kvA_{kv} + O(k^2, v^2). \tag{110}$$

For $O(1)$, we obtain

$$0 = (-1 + |\psi_0|^2 - \tilde{\boldsymbol{\nabla}}^2)\psi_0, \tag{111}$$

$$\left(\frac{1}{u}\tilde{\boldsymbol{\nabla}}^2 - |\psi_0|^2\right)\tilde{\varphi}_0 = -2\,\mathrm{Im}\,\hat{\boldsymbol{v}}_{\rm L}\cdot\psi_0\tilde{\boldsymbol{\nabla}}\psi_0^*, \tag{112}$$

and for $O(K)$

$$0 = -\psi_k + 2\psi_k|\psi_0|^2 + \psi_0^2\psi_k^* - \tilde{\boldsymbol{\nabla}}^2\psi_k + i\left(\tilde{\partial}_x^3 - 3\tilde{\partial}_x\tilde{\partial}_y^2\right)\psi_0, \tag{113}$$

$$\frac{1}{u}\tilde{\boldsymbol{\nabla}}^2\tilde{\varphi}_k - |\psi_0|^2\tilde{\varphi}_k - 2\,\mathrm{Re}\,(\psi_0\psi_k^*)\tilde{\varphi}_0 = 2\,\mathrm{Im}\,\hat{\boldsymbol{v}}_{\rm L}\cdot(\psi_0\tilde{\boldsymbol{\nabla}}\psi_k^* + \psi_k\tilde{\boldsymbol{\nabla}}\psi_0^*). \tag{114}$$

For $O(v_{\rm L})$, the equations are

$$\left(\hat{\boldsymbol{v}}_{\rm L}\cdot\tilde{\boldsymbol{\nabla}} - \frac{i}{2}\tilde{\varphi}_0\right)\psi_0 = -\psi_v + 2\psi_v|\psi_0|^2 + \psi_0^2\psi_v^* - \tilde{\boldsymbol{\nabla}}^2\psi_v, \tag{115}$$

$$\frac{1}{u}\tilde{\boldsymbol{\nabla}}^2\tilde{\varphi}_v - |\psi_0|^2\tilde{\varphi}_v - 2\,\mathrm{Re}\,(\psi_0\psi_v^*)\tilde{\varphi}_0 = 2\,\mathrm{Im}\,\hat{\boldsymbol{v}}_{\rm L}\cdot(\psi_0\tilde{\boldsymbol{\nabla}}\psi_v^* + \psi_v\tilde{\boldsymbol{\nabla}}\psi_0^*). \tag{116}$$

Finally, for $O(Kv_{\rm L})$

$$\begin{aligned}\hat{\boldsymbol{v}}_{\rm L}\cdot\tilde{\boldsymbol{\nabla}}\psi_k - \frac{i}{2}(\tilde{\varphi}_0\psi_k + \tilde{\varphi}_k\psi_0) &= -\psi_{kv} + \psi_0^2\psi_{kv}^* + 2\psi_{kv}|\psi_0|^2 + 2\psi_k\psi_0\psi_v^* + 2\psi_v\psi_0\psi_k^* \\ &\quad + 2\psi_k\psi_v\psi_0^* - \tilde{\boldsymbol{\nabla}}^2\psi_{kv} + i\left(\tilde{\partial}_x^3 - 3\tilde{\partial}_x\tilde{\partial}_y^2\right)\psi_v\end{aligned} \tag{117}$$

and

$$\begin{aligned}&\frac{1}{u}\tilde{\boldsymbol{\nabla}}^2\tilde{\varphi}_{kv} - |\psi_0|^2\tilde{\varphi}_{kv} \\ &\quad -2\,\mathrm{Re}\,(\psi_0\psi_{kv}^*\tilde{\varphi}_0 + \psi_0\psi_k^*\tilde{\varphi}_v + \psi_0\psi_v^*\tilde{\varphi}_k + \psi_k\psi_v^*\tilde{\varphi}_0) \\ &= 2\,\mathrm{Im}\,\hat{\boldsymbol{v}}_{\rm L}\cdot(\psi_0\tilde{\boldsymbol{\nabla}}\psi_{kv}^* + \psi_{kv}\tilde{\boldsymbol{\nabla}}\psi_0^* + \psi_k\tilde{\boldsymbol{\nabla}}\psi_v^* + \psi_v\tilde{\boldsymbol{\nabla}}\psi_k^*).\end{aligned} \tag{118}$$

The force balance relation becomes

$$\frac{\boldsymbol{j}_{\rm unif}\times\boldsymbol{\Phi}_0}{\Gamma v_{\rm L}|\Delta_\infty|^2} = \left[f_1 + kvf_2\begin{pmatrix}\hat{v}_{{\rm L}y} & \hat{v}_{{\rm L}x}\\ \hat{v}_{{\rm L}x} & -\hat{v}_{{\rm L}y}\end{pmatrix}\right]\hat{\boldsymbol{v}}_{\rm L} + O(k^2, v^2), \tag{119}$$

where f_1 and f_2 are linear and nonlinear coefficients in the force-velocity relation. The coefficient f_1 is a sum of the contributions from u-independent Tinkham mechanism (time dependence of amplitude of the gap) and u-dependent Bardeen-Stephen mechanism [25,29]. Here, the transverse friction force appears in addition to the longitudinal one. This form can be derived by a symmetry consideration, and has also been checked numerically.

The energy dissipation part can also be expanded with respect to k and v. In the dimensionless form, we can write it as

$$\tilde{w} = \frac{w}{\sigma_n\varphi_0^2/\xi^2} = 4u\left|\left(\hat{\boldsymbol{v}}_{\rm L}\cdot\tilde{\boldsymbol{\nabla}} + \frac{i}{2}\tilde{\varphi}\right)\psi\right|^2 + |\tilde{\boldsymbol{\nabla}}\tilde{\varphi}|^2. \tag{120}$$

The $O(v_{\rm L}K)$ component for $\tilde{w}$, or equivalently $O(v_{\rm L}^3K)$ for w, is responsible for the dissipation from nonreciprocal vortex dynamics.

Let us look at the spatial dependence of the above physical quantities. We use the two-dimensional polar coordinate $\boldsymbol{r} = (r,\phi)$ and the zeroth-order solution can be written as $\psi_0(\boldsymbol{r}) = f(r)e^{i\phi}$ for an isolated vortex. From the differential equation for ψ_0, we find the asymptotic behavior $f \propto r$ for $r \to 0$ and $f \to 1$ for $r \to \infty$ [29]. Among functional forms that satisfy

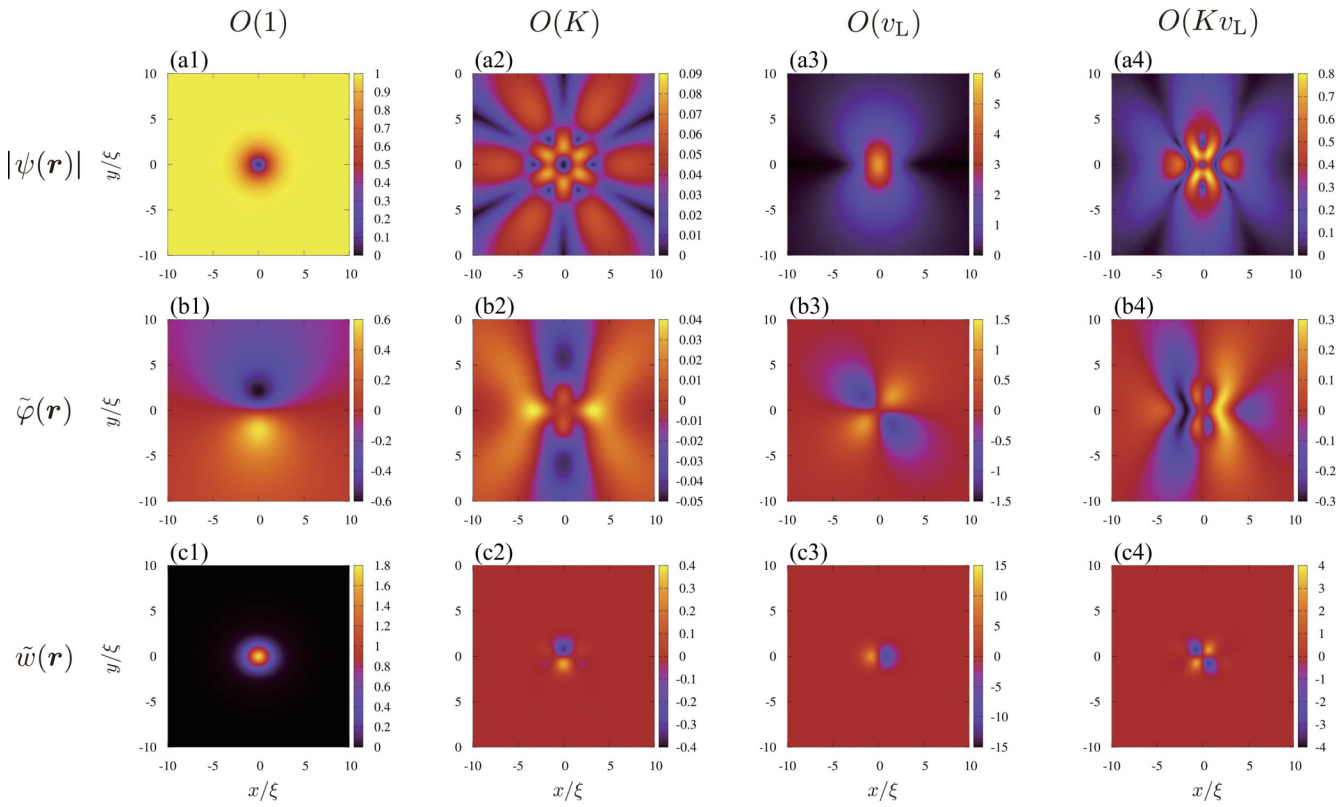

FIG. 2. Spatial dependencies of the amplitude of wave functions, scalar potential, and energy dissipation rate: (a1) $|\psi_0|$, (a2) $|\psi_k|$, (a3) $|\psi_v|$, (a4) $|\psi_{kv}|$; (b1) $\tilde{\varphi}_0$, (b2) $\tilde{\varphi}_k$, (b3) $\tilde{\varphi}_v$, (b4) $\tilde{\varphi}_{kv}$; (c1) $\tilde{w}_0$, (c2) $\tilde{w}_k$, (c3) $\tilde{w}_v$, (c4) $\tilde{w}_{kv}$. We have chosen $\boldsymbol{v}_{\rm L} = v_{\rm L}\hat{\boldsymbol{x}}$ and used $u = 1$ (i.e., $\ell_E = \xi$). The system size is $L \times L$ with $L = 40\xi$ and the number of mesh is $N_L \times N_L$ with $N_L = 300$.

these limiting behaviors, we choose $f(r) = \tanh(ar/\xi)$ and the constant is determined as $a = \sqrt{\frac{3}{8}}$ by using the differential equation at small r. Then, the physical quantities such as $\psi_{0,k,v,kv}$, $\tilde{\varphi}_{0,k,v,kv}$, and $\tilde{w}_{0,k,v,kv}$ are numerically calculated by solving the linear differential equations derived above.

Figures 2(a1)–2(a4) show the spatial dependencies of the amplitudes of gap functions. The originally circular shape in Fig. 2(a1) is modified by K and $v_{\rm L}$, and sixfold and twofold patterns appear in Figs. 2(a2) and 2(a3), respectively. The more complex pattern is seen in the higher-order contribution ψ_{kv} [Fig. 2(a4)]. The scalar potentials are also shown in Figs. 2(b1)–2(b4). The dipolar field is generated in φ_0 which causes the electric field inside the normal core. We note that the dimensionless $\tilde{\varphi}_0$ is $O(1)$ but the scalar potential φ_0 is $O(v_{\rm L})$ contribution. Then, φ_v shown in Fig. 2(b3) is an $O(v_{\rm L}^2)$ contribution, having the quadrupolar distribution. The situation is further modified in the presence of the cubic term as in Figs. 2(b2) and 2(b4). We show in Figs. 2(c1)–2(c4) the energy dissipation rate as a function of spatial coordinates. The dissipation occurs in the region with $r \lesssim \ell_E$ as shown in Fig. 2(c1) [note that W_0 is an $O(v_{\rm L}^2)$ contribution]. This also applies at higher orders shown in Figs. 2(c2)–2(4), where the spatial anisotropy is introduced.

We are also interested in the parameter $u = \xi^2/\ell_E^2$ dependence of the physical quantities. Figure 3 shows the force coefficients f_1 and f_2 as a function of u. For the larger u, meaning shorter electric-field penetration length, the value of f_1 becomes smaller. This is because the region where the dissipation occurs shrinks to make a weaker friction force. The value of f_2 at sufficiently large u also becomes small due to the same reason as f_1. On the other hand, f_2 at small u decreases in contrast with f_1. While the reason for the behavior is not easily understood in an intuitive way, in any case we have here confirmed that the coefficients of f_1 and f_2 are order of unity in the experimentally relevant regime with $u \sim 1$.

3. *Flux-flow conductivity*

Using the relation $\boldsymbol{E}_0 = \boldsymbol{B} \times \boldsymbol{v}_{\rm L}$ for an electric field generated by the motion of the magnetic flux, which is derived from

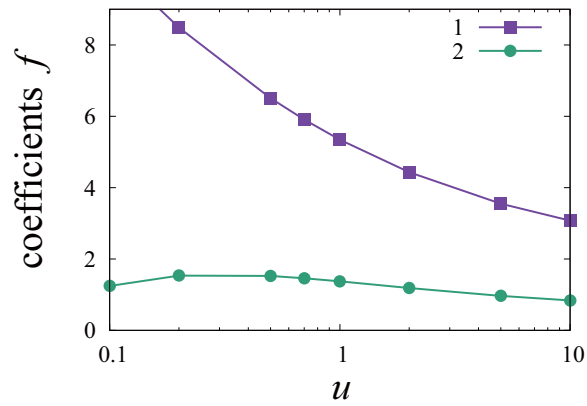

FIG. 3. Parameter u dependence of the friction force coefficients defined in Eq. (119). The system size and number of spatial mesh are same as Fig. 2.

the Josephson relation, we obtain the electrical conductivity as

$$\boldsymbol{j}_{\rm unif} = \frac{\Gamma|\Delta_\infty|^2}{\Phi_0 B_z}\left[f_1 + \frac{f_2 \Gamma K}{|\alpha|^2\xi^4 B_z}\begin{pmatrix} E_{0x} & -E_{0y} \\ -E_{0y} & -E_{0x}\end{pmatrix}\right]\boldsymbol{E}_0 \tag{121}$$

$$= \sigma_{1\rm v}\boldsymbol{E}_0 + \sigma_{2\rm v}\boldsymbol{F}(\boldsymbol{E}_0), \tag{122}$$

where the vector $\boldsymbol{F}$ is same as that in Eq. (59). To express the flux-flow conductivity in terms of normal conductivity, we use the electric field penetration depth ℓ_E and the upper critical field given by $B_{c2} = \Phi_0/2\pi\xi^2$. Then, the conductivities are written as

$$\sigma_{1\rm v} = \frac{u f_1(u)}{4\pi}\sigma_n \frac{B_{c2}}{B_z}, \tag{123}$$

$$\sigma_{2\rm v} = \frac{u f_2(u)}{4\pi}\sigma_n \frac{B_{c2}\Gamma K}{\gamma^2 B_z^2}. \tag{124}$$

The γ value from nonreciprocal vortex dynamics is given by

$$\gamma_{\rm S}^{\rm v} = \frac{\sigma_{2\rm v}}{\sigma_{1\rm v}^2 B_z W} = \frac{4\pi f_2(u)}{u f_1(u)^2}\frac{\Gamma K}{\gamma^2 \sigma_n B_{c2} B_z W}. \tag{125}$$

This expression does not depend on B_z since K is proportional to B_z due to the Zeeman effect. We note that the parameters σ_n, γ, and K are in general dependent on the purity of the sample (see Appendix B).

Let us compare this result with the γ value ($\gamma_{\rm S}^{\rm f}$) from superconducting fluctuation for $T \gtrsim T_0$ given by Eq. (60) [10]. Noting $u \sim 1$, the ratio is estimated by

$$\frac{\gamma_{\rm S}^{\rm v}}{\gamma_{\rm S}^{\rm f}} \sim \frac{T_0^2}{E_{\rm F}(T_0 - T)}. \tag{126}$$

Thus, we obtain the same conclusion as the extended Bardeen-Stephen approach in Sec. III A 2.

C. Ratchet motion of vortex

As discussed above, for $T < T_0$ and in the presence of the finite out-of-plane magnetic field, the motion of quantum vortices penetrating the superconductor gives a dominant contribution to the voltage drop. Here, we consider another effect for vortex dynamics. In the superconductor without inversion center, vortices driven by the external charge current feel an asymmetric pinning potential acting on them (ratchet effect). This effect has been proposed to control the vortices in superconductors [32–34]. New perspective here is that the vortex ratchet effect *naturally* appears as a consequence of disorders in noncentrosymmetric system, which is distinct from the previously discussed *artificially* developed inversion-broken environment. In this section, we analyze the classical motion of vortices under the asymmetric periodic potential and discuss the nonreciprocal transport there. The relevant parameters such as potential height and its spatial periodicity are estimated from pinning properties such as a magnitude of the critical current density where the vortices are depinned. The relation to the recent experimental results [10,35] will also be discussed in Sec. IV C 2. The classical equation of motion of the vortices in the diffusive limit is modeled as

$$\eta\frac{dx}{dt} = -\frac{\partial U}{\partial x} + F - \sqrt{2\eta T}\xi(t), \tag{127}$$

with U being the pinning potential, which we here assume to be periodic for simplicity: $U(x + L) = U(x)$, and F is the uniform force. The last term is the Langevin force with zero mean and unit dispersion (Gaussian white noise). η is the viscous friction coefficient, and T is the temperature. By solving the corresponding Fokker-Planck equation

$$\frac{\partial p}{\partial t} = \frac{1}{\eta}\frac{\partial}{\partial x}\left[\left(\frac{\partial U}{\partial x} - F\right)p + T\frac{\partial p}{\partial x}\right] \tag{128}$$

for the distribution function $p(x, t)$, we obtain the steady velocity of the vortex after long time expressed as [36]

$$v_{\rm L} = \frac{L}{\beta\eta}\frac{1 - e^{-\beta F L}}{\int_0^L dy\, I_0(y) e^{-\beta F y}}, \tag{129}$$

where we have introduced

$$I_0(y) = \int_{x_0}^{x_0+L} dx\, e^{\beta[U(x)-U(x-y)]}, \tag{130}$$

with $\beta = 1/T$ being the inverse temperature. We can choose x_0 arbitrarily due to the periodicity of the potential. Potential is called symmetric when there exists certain choice of $x_0 \in [0, L)$ such that $U(x) = U(x_0 - x)$ is satisfied. Here, we can choose $x_0 = 0$ by shifting the x coordinate. By using the evenness and the periodicity of the potential, we can easily prove $v_{\rm L}(-F) = -v_{\rm L}(F)$ which show the absence of the nonreciprocal transport.

For asymmetric potentials, the situation is different. The velocity $v_{\rm L}$ is expanded with respect to the force F as

$$v_{\rm L} = q_1 F + q_2 F^2 + O(F^3), \tag{131}$$

where the coefficients are

$$q_1 = \frac{L}{\beta\eta}\frac{\beta L}{\int_0^L dy\, I_0(y)}, \tag{132}$$

$$q_2 = \frac{L}{\beta\eta}\frac{\beta^2 L\int_0^L dy\left(y - \frac{L}{2}\right)I_0(y)}{\left[\int_0^L dy\, I_0(y)\right]^2}, \tag{133}$$

where q_2, which is a hallmark of the nonreciprocal transport, survives only for asymmetric potentials as discussed above.

Hereafter, we adopt the fully asymmetric periodic potential for simplicity

$$U(x) = U_0\,\mathrm{saw}\left(\frac{x}{L}\right) = U_0\frac{x}{L} \pmod L \tag{134}$$

by using so-called sawtooth function. $U_0(>0)$ is the height of the pinning potential. In this potential, the steady velocity is calculated as

$$v_{\rm L} = \frac{1}{\beta\eta L}\frac{\beta^2(U_0 - FL)^2}{\beta FL - \beta U_0 - \sinh(\beta U_0) + [\cosh(\beta U_0) - 1]\coth\left(\frac{\beta FL}{2}\right)} = q_1 F + q_2 F^2 + O(F^3), \tag{135}$$

with the response coefficients

$$q_1 = \frac{1}{2\eta}\frac{\beta^2 U_0^2}{\cosh(\beta U_0)-1} = \begin{cases} \frac{1}{\eta} - \frac{\beta^2 U_0^2}{12\eta} & (\beta U_0 \to 0), \\ \frac{\beta^2 U_0^2}{\eta} e^{-\beta U_0} & (\beta U_0 \to \infty) \end{cases} \tag{136}$$

and

$$q_2 = \frac{L\beta}{4\eta}\frac{\beta^3 U_0^3 + \beta^2 U_0^2 \sinh(\beta U_0) + 4\beta U_0 - 4\beta U_0 \cosh(\beta U_0)}{[\cosh(\beta U_0)-1]^2} = \begin{cases} \frac{L}{\eta}\frac{\beta^4 U_0^3}{360} & (\beta U_0 \to 0), \\ \frac{L}{\eta}\frac{\beta^3 U_0^2}{2} e^{-\beta U_0} & (\beta U_0 \to \infty). \end{cases} \tag{137}$$

Since the voltage drop originating from the motion of vortices is $V = B_z L_x v_L$ and the force acting on vortices is $F = \frac{\phi_0}{W} I$, we can calculate the coefficients in current-voltage relation [Eq. (4)] as $a_1(B_z, T) = \phi_0 \frac{L_x}{W} B_z q_1(T)$ and $a_2(B_z, T) = \phi_0^2 \frac{L_x}{W^2} B_z q_2(T)$, both of which are proportional to B_z. The nonreciprocal γ' parameter defined as $R = R_0(1 + \gamma' I)$ with $V = RI$ is expressed as

$$\begin{aligned} \gamma' &= \frac{q_2}{q_1}\frac{\phi_0}{W} \\ &= \frac{\phi_0 L}{W}\frac{U_0^2\beta^2 + \beta U_0 \sinh(\beta U_0) - 4\cosh(\beta U_0) + 4}{4U_0 \sinh^2\left(\frac{\beta U_0}{2}\right)} \\ &= \begin{cases} \frac{\phi_0 L}{W}\frac{\beta^4 U_0^3}{360} & (\beta U_0 \to 0), \\ \frac{\phi_0 L}{W}\frac{\beta}{2} & (\beta U_0 \to \infty), \end{cases} \end{aligned} \tag{138}$$

which monotonically decreases as raising temperature. Note that the exponential temperature dependence vanishes for the γ value.

In this calculation, we have neglected the vortex-vortex interaction. This assumption is justified for small magnetic field where the vortices are dilute enough. We also note that the ratchet effect is active for trigonal symmetry, but is not relevant for the systems with C_∞ and hexagonal symmetries where no ratchet potential is present. In the latter cases, the effect from asymmetric spin-orbit coupling plays the central role.

IV. DISCUSSION

Here, we discuss expected nonreciprocal charge transport signals in 2DNS. Table I summarizes the nonreciprocal I-V characteristics in Rashba superconductors, TI surface and TMD for both above and below transition temperature. The magnetic fields are applied parallel to the two-dimensional plane for Rashba and TI-based systems, and applied perpendicular to the layer for TMD. While the other configurations can in principle be possible, the information of this paper gives a firm basis to explore the further properties. Below we discuss each system separately.

A. Rashba superconductors

Here, we consider the γ value for Rashba superconductors. With electron or hole doping, the Fermi energy can be tuned and the behavior is dependent on the sign of E_F. Let us begin with the $E_F < 0$ case. In this case, the normal contribution to γ value becomes finite as shown in Ref. [9] (see also Table I). The typical values for BiTeBr have been estimated [9] by using the effective mass $m = 0.15m_e$, the Rashba parameter $\alpha = 2.00$ eV Å, and the g factor $g = 60$. In the normal state with $E_F = -0.01$ eV, the amplitude of the magnetochiral anisotropy is estimated as $W\gamma_N \simeq 2 \times 10^{-5}$ T^{-1} A^{-1} m.

The system crosses over into the paraconductivity region with approaching to the mean field transition temperature T_0 from above. Here, as discussed in Sec. II A, the parity mixing contribution becomes irrelevant and the cubic term in GL free energy instead becomes dominant. The paraconductivity is then given by Eq. (37). The ratio between normal and superconducting states is given by $\gamma_S/\gamma_N \sim E_F/T_0$, and thus the nonreciprocal signal is strongly enhanced by the appearance of a small energy scale T_0 for superconductors.

The fluctuation contribution above T_0 further crossovers to vortex contribution at lower temperatures than T_0. Below T_0, the pair amplitude sufficiently develops and the free vortices, which are generated thermally above KT transition temperature in the present system, start to play an important role for transport phenomena. For $E_F < 0$ case, the cubic term effectively renormalizes superfluid density under the transport current as discussed in Sec. III A. As a result, the friction force and KT transition temperature are modified and have different values depending on the direction of source currents. The former causes the characteristic temperature dependence in the γ value as $\gamma_S \propto (T_0 - T)^{-1}$ near T_0 ($> T_{KT}$). Note that this expression smoothly connects to the fluctuation contribution for $T > T_0$, and does not show divergence in reality. On the other hand, the modification of the KT transition temperature shows the divergent γ value as $\gamma_S \propto (T - T_{KT})^{-3/2}$ near the KT transition point. For $T < T_{KT}$, vortex and antivortex are bound, and the linear transport coefficient finally vanishes. The third-order term with a_3 then becomes the relevant one in the current-voltage relation. The nonreciprocity is reflected in the higher-order term with a_4 in this case. More detailed investigation of these higher-order contributions remains to be clarified in the future.

Now, we switch our focus to the $E_F > 0$ case. Although the normal-state contribution to γ value is absent in this situation [9], the paraconductivity is finite. There are two contributions to paraconductivity: one from parity mixing and the other from $\boldsymbol{q}$-cubic term in the GL theory. Here, as the ratio is calculated in Eq. (38), the parity-mixing contribution in Eq. (23) is much larger than the other. The γ value in this case has been estimated in Ref. [18] for BiTeBr with superconducting proximity effects. On the othe hand, the $LaAlO_3/SrTiO_3$ interface [37–40] is also a typical two-dimensional Rashba superconductor. Its carrier density is given by $n \sim 10^{13}$ cm^{-2}, spin-orbit field is

$B_{SO} = \frac{m^2\alpha^2}{|e|} \sim 1$ T, the Debye temperature is $T_D \sim 400$ K, and the mean field transition temperature is $T_0 \sim 100$ mK. If we assume $r_t = 0.1$ and the typical sample width $W = 10^{-6}$ m, the γ value is estimated as $\gamma_S \sim 8 \times 10^4$ T^{-1} A^{-1}, which is much larger than the previous studies [3,5–8].

At lower temperature below T_0, the vortex contribution dominates over the paraconductivities. For $E_F > 0$ case, the two-component gap parameter needs to be considered for vortex dynamics. While detailed studies remain unexplored, the vortex contribution should be present and is expected to cause a singular behavior around the KT transition point as in the $E_F < 0$ case.

B. TI surface

We here discuss the surface of topological insulators plus superconducting proximity effect. The Hamiltonian has the $\boldsymbol{k}$-linear term, but the nonreciprocal charge transport is absent with this term only since magnetic field just shifts the wave vector. We have thus considered the two more terms to generate the nonreciprocity: parabolic term and hexagonal warping term. Let us first consider the paraconductivity contribution from parabolic term based on Eq. (43). The functional forms of the γ values are listed in Table I, and the ratio between normal and superconducting states is given by $\gamma_S/\gamma_N \sim E_F/T_0$. Hence, the nonreciprocal transport signal is enhanced in superconducting state. To estimate the typical value, we use the expression in Eq. (43) with $\hbar$, k_B, and μ_B recovered. If we assume $v_F = 2.84$ eV Å and $\frac{1}{2m} = 41.1$ eVÅ^2 in Bi_2Te_3 [41], and $E_F = 0.1$ eV, $T_0 = 10$ K, and $W = 100$ μm as typical values, we obtain $\gamma_S \approx 0.33$ A^{-1} T^{-1}. On the other hand, the contribution from the hexagonal warping is given in Eq. (53), which is also estimated here. Assuming the same parameters above and $\sqrt{\lambda} = 250$ eVÅ^3 in Bi_2Te_3 [22,41], we obtain $\gamma_S \approx 0.11$ A^{-1} T^{-1}. Therefore, the amplitude is comparable to that by the parabolic term.

At lower temperatures, the vortex contribution becomes dominant as in the Rashba superconductors. Since the magnetic field is applied along the two-dimensional plane and there is the cubic term in GL free energy, the behavior is essentially same as the Rashba superconductors with $E_F < 0$. Namely, the thermally generated vortex in the $T_{KT} < T \lesssim T_0$ region creates the characteristic magnetochiral anisotropy in the forms $\gamma_S \propto (T_0 - T)^{-1}$ for $T \to T_0$ and $\gamma_S \propto (T - T_{KT})^{-3/2}$ for $T \to T_{KT}$. We note that the above transport coefficients are written in the form $V = a_1 I(1 + \gamma BI)$, i.e., the magnetic field B enters only with γ value. As shown below, however, the situation can qualitatively change if the magnetic field is applied perpendicular to the plane.

C. TMD

1. Paraconductivity and intrinsic vortex-flow contribution

We estimate the physical quantities of the clean MoS_2. Let us begin with the normal contribution well above T_0. This system has a valley degrees of freedom, whose contribution to the normal γ value per valley is listed in Table I. With the situation in MoS_2, however, the γ value for each valley has different sign and vanishes if we sum up both the contributions [10]. Near T_0, the paraconductivity contribution is developed as given in Eq. (60). Using $2m\lambda/\hbar^2 = -0.49$ and $\Delta_{SO} \simeq 7.5$ meV, and $T_0 = 8.8$ K for monolayer MoS_2, the γ value from the superconducting fluctuation reaches $\gamma_S \simeq 250$ T^{-1} A^{-1} for the sample width $W \simeq 3\,\mu$m, as shown in Ref. [10].

Below T_0, here again the vortex contribution becomes relevant for the γ value, but the situation is different from the Rashba and TI-based systems with KT transition. Namely, the vortices with the same vorticity are induced by the out-of-plane magnetic field and the KT transition is washed away for $B \neq 0$. As a result, the number of vortices is determined by the external field B, and the ordinary resistivity $a_1(B)$ is proportional to B. We reflect this situation by denoting I-V characteristic as $V = a_1' BI + a_2(B)I^2$. As for the coefficient $a_2(B)$, there are two types of contributions. One is from the $\boldsymbol{q}$-cubic term in the GL free energy and a_2 is proportional to B^2. The other is from the ratchet potential for vortices, and $a_2 \propto B$ is satisfied. Thus, the B dependence of a_2 clearly distinguishes the underlying mechanism to generate nonreciprocal charge transport. Since the latter effect is discussed in detail in the next subsection, we here focus on the cubic-term contribution. The I-V relation is then written as $V = a_1' BI(1 + \gamma_S BI)$.

As discussed in Sec. III A, the $\boldsymbol{q}$-cubic term in GL free energy effectively renormalizes the superfluid density. We have applied the generalized Bardeen-Stephen approach to this system: the force balance between driving (Magnus) force and viscous force acting on the vortex is considered. The nonreciprocity enters in the friction force through the anisotropically renormalized superfluid density. We have then found that the γ value from vortex dynamics is given by $\gamma_S^v = \gamma_S^f \times \frac{T_0^2}{E_F(T-T_0)}$ with γ_S^f being the superconducting fluctuation contribution, which has a large value near the mean-field transition temperature T_0. Here, the temperature dependence enters through the unrenormalized superfluid density which behaves as $n_s \propto (T_0 - T)$. Such behavior has further been justified by the TDGL approach as demonstrated in Sec. III B. If the results are extrapolated to zero temperature, we get $\gamma_S^v/\gamma_S^f = T_0/E_F$. Since the magnitude of the paraconductivity contribution is roughly given by $\gamma_S^f \sim 10^2$ T^{-1} A^{-1} as discussed above, the order of magnitude for the vortex contribution is $\gamma_S^v \sim 1$ T^{-1} A^{-1} in the low-temperature limit. This is much smaller than the observed values at low T in the monolayer MoS_2 [10], and hence we need another mechanism to account for the experimental results.

2. Ratchet effect of vortex flow

We now consider the nonreciprocal transport from ratchet effect of vortex dynamics based on Eq. (138). Phenomenological parameters such as periodicity L of the pinning potential, friction coefficient η, and potential height U_0 are estimated for MoS_2 using experimental data. The parameter L is determined from the mean distance of pinning centers. This can be estimated from pinning-depinning transition point in the magnetoresistance measurement, that is about $B_z \simeq 0.2$ T [35]. At this transition point, all the pinning centers are assumed to be filled with vortices. The total flux is $B_z L_x W = N_v \Phi_0$ and then the vortex number density is $n_v = N_v/(L_x W) = B_z/\Phi_0$. Thus, the mean distance between vortices is

$$L \sim \frac{1}{\sqrt{n_v}} = \sqrt{\frac{\Phi_0}{B_z}} \sim 10^{-7}\ \text{m}. \tag{139}$$

The parameter η is estimated by the normal-state resistivity. In the absence of the pinning potentials (i.e., $U_0 = 0$), the I-V characteristic becomes $v_{\rm L} = F/\eta$ or

$$V = B_z v_{\rm L} L_x = B_z \frac{F}{\eta} L_x = B_z \frac{\Phi_0}{\eta} \frac{L_x}{W} I = RI \tag{140}$$

in the Ohmic region. The resistivity $R = B_z \frac{\Phi_0}{\eta} \frac{L_x}{W}$ should be same as the normal-state resistivity R_n when $B_z = B_{\rm c2} \simeq 0.1$ T. Thus, the parameter η is estimated as

$$\eta = \frac{\Phi_0 B_{\rm c2}}{R_n} \frac{L_x}{W} = \frac{\Phi_0 B_{\rm c2}}{R_n} \sim 10^{-18}\ {\rm kg/s}, \tag{141}$$

with $R_{n,\rm sheet} \simeq 300\ \Omega$ [42].

The parameter U_0, the height of the pinning potential of the superconducting vortex, is estimated by the plateau of R-B curve in weak B region. The plateau disappears for $j_{\rm sheet} > j_{\rm c} \simeq 3$ A/m [35], where $j_{\rm c}$ is the critical current density for vortex depinning. Depinning transition occurs when the pinning potential is well tilted by the external force, namely,

$$U_0 \sim FL = j_{\rm sheet} \Phi_0 L \simeq 4\ {\rm meV}. \tag{142}$$

Another estimation of U_0 is from the thermodynamic upper critical field. The vortex energy per unit volume is $B_{c2}^2/(2\mu_0)$. When the vortex has the overlap with normal core in the pinning center, the energy reduces. By using $B_{c2} \simeq 0.1$ T [42], we obtain

$$U_0 \sim \frac{B_{c2}^2}{2\mu_0} \pi \xi^2 c_z \simeq 5\ {\rm meV}, \tag{143}$$

with $\xi \simeq 8$ nm and $c_z \simeq 1$ nm being the in-plane coherence length (normal core radius) and the lattice constant in the thickness direction, respectively. These two estimations are very consistent. We note $U_0 \simeq 5$ meV $\simeq 58$ K is much larger than the transition temperature, therefore the low-temperature limit $\beta U_0 \gg 1$ is the realistic situation in MoS_2.

Calculated I-V characteristic curve is shown in Fig. 4, which displays a strong rectification behavior even at a measurable temperature. For larger current such that $U_0 < FL$, the expansion with respect to F or equivalent to I is no longer valid. In this regime, the I-V characteristics are strongly non-linear and hence the higher harmonics becomes relevant. At the critical current where $U_0 = F_c L$, the potential becomes a multistep function and therefore the velocity begins to grow rapidly.

The temperature dependence of γ value at low T is given by $\gamma_{\rm S}' \propto 1/T$ for the ratchet mechanism according to Eq. (138) in the $U_0 \gg T$ limit. With the original expression in Eq. (138), the estimated γ values for the sample size $L_x W c_z = 3\ \mu{\rm m} \times 3\ \mu{\rm m} \times 1$ nm are given by $\gamma_{\rm S}' \simeq 8 \times 10^5\ {\rm A}^{-1}$ at $T = 10$ K and $\gamma_{\rm S}' \simeq 1 \times 10^6\ {\rm A}^{-1}$ at $T = 2$ K. Although these magnitudes are much larger than the ones in the experimental observation [10], we can obtain the more close values by controlling the spatial asymmetry in the sawtooth potential. Namely, by tuning the potential from the asymmetric case in Eq. (134) to symmetric case continuously, the γ value is monotonically decreased down to zero.

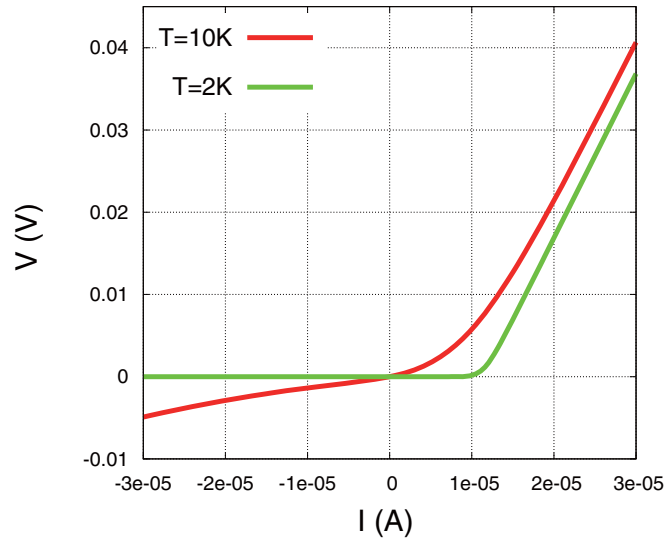

FIG. 4. I-V characteristic curve for the monolayer MoS_2 at $T = 10$ K and $T = 2$ K.

At sufficiently low temperatures, on the other hand, the quantum nature of the vortices plays an important role. In this case, the wave character of vortices appears, which will modify the above physical picture. This point remains to be explored in the future.

V. SUMMARY AND CONCLUSIONS

We have theoretically investigated the nonreciprocal charge transports in the two-dimensional superconductors without inversion symmetry. We have taken the concrete examples such as the Rashba superconductors and topological insulator surface with in-plane magnetic fields, and the monolayer transition-metal dichalcogenide (MoS_2) with out-plane magnetic field. The nonreciprocal properties of superconductors are reflected in the I-V characteristics with the form $V = a_1 I + a_2 I^2 + a_3 I^3 + a_4 I^4$, and the even-order terms represent the nonreciprocal responses. These coefficients are clarified in the temperature range both above and below the mean field transition temperature. Table I summarizes our obtained results.

The nonreciprocal transport signals in the normal regions well above the mean field transition temperature T_0 cross over into superconducting fluctuation contribution (paraconductivity). We have newly investigated the topological-insulator-based systems which have cubic term in the GL free energy, in addition to the previously investigated Rashba superconductors and transition-metal dichalcogenide. The γ values for all the systems are much enhanced compared to the normal state, which is attributed to the appearance of the small energy scale T_0 ($\ll E_{\rm F}$). The ratio of γ values between normal and superconducting fluctuation regions is in general written as $(E_{\rm F}/T_0)^m$ with $m \geqslant 1$ being an integer depending on the system.

Below T_0, the amplitude of the superconducting order parameters is developed and only the phase degrees of freedom are left. Then, the vortex dynamics plays an important role for $T \lesssim T_0$. There are two different kinds of vortex

behaviors. First, for systems with in-plane magnetic fields, the vortices are thermally generated and are bound below the Kosterlitz-Thouless transition temperature $T_{\rm KT}$. Due to the inversion symmetry breaking in the system, the friction force and the number of vortices for $T_{\rm KT} < T < T_0$ are different depending on the direction of external uniform current, to produce the nonreciprocal charge transport. These effects have effectively been described by the renormalization of the superfluid density. The γ value, which is defined by $V = a_1 I(1+\gamma BI)$ as in the fluctuation regime, is identified to have the temperature-dependent forms $\gamma \propto (T_0 - T)^{-1}$ near T_0 and $\gamma \propto (T - T_{\rm KT})^{-3/2}$ near $T_{\rm KT}$, which originate from the modified friction coefficient and the modified KT transition temperature, respectively. Accordingly, we expect the two-peak structure of the temperature dependence of the γ value in this case.

For the system with out-plane magnetic field, the number of vortices with a same vorticity is determined by the strength of the external field B and the Kosterlitz-Thouless transition does not exist. The nonreciprocal signal γ is now characterized by the I-V relation with the form $V = a_1' BI(1+\gamma BI)$. The renormalization of superfluid density works also for this system, and we have derived the modified friction force for moving vortices and the corresponding γ value has the form $\gamma \propto (T_0 - T)^{-1}$. This phenomenological approach is further justified by the time-dependent Ginzburg-Landau theory. On the other hand, we have also investigated the other effect with ratchet potential for vortices. Here, the magnetic field plays a role only for creating the vortex, and then the γ value is characterized by the relation $V = a_1' BI(1+\gamma' I)$. We have considered one-dimensional motion driven by the external transport current in the sawtooth potential, and have found that the resultant signal γ' can have a comparable value with the experiments in MoS_2.

We have thus systematically clarified the characteristic transport properties for two-dimensional noncentrosymmetric superconductors. The knowledge of this paper is useful for the further exploration of nonreciprocal phenomena in superconductors both theoretically and experimentally.

ACKNOWLEDGMENTS

We are grateful to Y. Saito, T. Ideude, Y. Itahashi, and Y. Iwasa for fruitful discussions. S.H. acknowledges Yusuke Kato for useful conversation on vortex dynamics. R.W. was supported by the Grants-in-Aid for Japan Society for the Promotion of Science (JSPS) Grant No. JP15J09045. K.H. was supported by JSPS through a research fellowship for young scientists and the Program for Leading Graduate Schools (MERIT). N.N. was supported by JSPS KAKENHI Grants No. JP26103006 and No. JP18H03676, and Core Research for Evolutional Science and Technology (CREST), Japan Science and Technology Agency (JST) (Grant No. JPMJCR16F1).

APPENDIX A: DERIVATION OF THE GINZBURG-LANDAU FREE ENERGY

Following Ref. [20], we derive the GL free energy for the model in Eq. (7). Especially, we focus on the case where the Fermi energy is on the conduction band. The free energy is given by

$$F = \int \frac{d^2\boldsymbol{q}}{(2\pi)^2}\left[\frac{1}{g} - T\sum_{\omega_n}\int \frac{d^2\boldsymbol{k}}{(2\pi)^2} G(\boldsymbol{k}, i\omega_n) \times G(-\boldsymbol{k}+\boldsymbol{q}, -i\omega_n)\right]|\Delta_{\boldsymbol{q}}|^2, \tag{A1}$$

with $G(\boldsymbol{k}, i\omega_n) = (i\omega_n - \xi_{\boldsymbol{k}})^{-1}$ being the Matsubara Green's function [$\omega_n = (2n+1)\pi T$]. The product of the Green functions is simplified as

$$\int \frac{d^2\boldsymbol{k}}{(2\pi)^2} G(\boldsymbol{k}, i\omega_n) G(-\boldsymbol{k}+\boldsymbol{q}, -i\omega_n) = -\int \frac{d^2\boldsymbol{k}}{(2\pi)^2} \frac{1}{i\omega_n - \xi_{\boldsymbol{k}}^0 - \Omega_1(\boldsymbol{k})} \frac{1}{i\omega_n + \xi_{\boldsymbol{k}}^0 + \Omega_2(\boldsymbol{k}, \boldsymbol{q})}, \tag{A2}$$

where

$$\xi_{\boldsymbol{k}}^0 = \frac{\boldsymbol{k}^2}{2m} + \alpha|\boldsymbol{k}| - E_{\rm F}, \tag{A3}$$

$$\Omega_1(\boldsymbol{k}) = \xi_{\boldsymbol{k}} - \xi_{\boldsymbol{k}}^0, \tag{A4}$$

$$\Omega_2(\boldsymbol{k}, \boldsymbol{q}) = \xi_{-\boldsymbol{k}+\boldsymbol{q}} - \xi_{\boldsymbol{k}}^0. \tag{A5}$$

We first integrate by $\xi_{\boldsymbol{k}}^0$:

$$\begin{aligned} &-\int \frac{d^2\boldsymbol{k}}{(2\pi)^2} \frac{1}{i\omega_n - \xi_{\boldsymbol{k}}^0 - \Omega_1(\boldsymbol{k})} \frac{1}{i\omega_n + \xi_{\boldsymbol{k}}^0 + \Omega_2(\boldsymbol{k}, \boldsymbol{q})} \\ &\approx -\nu_1 \left\langle \int d\xi \frac{1}{i\omega_n - \xi - \Omega_1(\boldsymbol{k})} \frac{1}{i\omega_n + \xi + \Omega_2(\boldsymbol{k}, \boldsymbol{q})} \right\rangle_{\boldsymbol{k}} \\ &= \pi\nu_1 \left\langle \frac{1}{|\omega_n| + i\,\mathrm{sgn}(\omega_n)\Omega(\boldsymbol{k}, \boldsymbol{q})} \right\rangle_{\boldsymbol{k}}, \end{aligned} \tag{A6}$$

where $\langle \dots \rangle_{\boldsymbol{k}}$ is the momentum average over the Fermi surface. We have defined $\Omega(\boldsymbol{k}, \boldsymbol{q}) = \frac{1}{2}[\Omega_1(\boldsymbol{k}) - \Omega_2(\boldsymbol{k}, \boldsymbol{q})]$. When we consider the surface state of topological insulator, which we describe here for simplicity, we only take the inner one of the two Fermi surfaces. The Fermi wave number is $k_{\rm F1} = -m\alpha + \sqrt{mE_{\rm FR}}$, and the density of states is $\nu_1 = \frac{m}{2\pi}(1 - \alpha\sqrt{m/E_{\rm FR}})$. Therefore, the second term in Eq. (A1) is

$$\begin{aligned} &-\pi T\nu_1 \sum_{\omega_n} \left\langle \frac{1}{|\omega_n| + i\,\mathrm{sgn}(\omega_n)\Omega(\boldsymbol{k}, \boldsymbol{q})} \right\rangle_{\boldsymbol{k}} \\ &\approx -\pi T\nu_1 \sum_{\omega_n} \left\langle \frac{1}{|\omega_n|} - \frac{\Omega(\boldsymbol{k}, \boldsymbol{q})^2}{|\omega_n|^3} + \frac{\Omega(\boldsymbol{k}, \boldsymbol{q})^4}{|\omega_n|^5} \right\rangle_{\boldsymbol{k}} \\ &= -\nu_1[S_1(T) - S_3(T)\langle\Omega(\boldsymbol{k}, \boldsymbol{q})^2\rangle + S_5(T)\langle\Omega(\boldsymbol{k}, \boldsymbol{q})^4\rangle], \end{aligned} \tag{A7}$$

with $S_k(T) = \pi T \sum_n |\omega_n|^{-k}$. The functions $S_1(T)$ and $S_3(T)$ are given in Eqs. (17) and (18), and $S_5(T)$ is calculated as

$$S_5(T) = \frac{31\zeta(5)}{16(\pi T)^4}. \tag{A8}$$

Then, we calculate $\langle\Omega(\boldsymbol{k},\boldsymbol{q})^2\rangle$ and $\langle\Omega(\boldsymbol{k},\boldsymbol{q})^4\rangle$ up to $O(B_y\boldsymbol{q}^4)$. If we shift the momentum as $\boldsymbol{q}\to\boldsymbol{q}+\frac{2B_y m}{|\boldsymbol{k}|+m\alpha}\hat{\boldsymbol{x}}$, we find

$$\langle\Omega(\boldsymbol{k},\boldsymbol{q})^2\rangle = \frac{(k_{\rm F1}+m\alpha)^2}{8m^2}\boldsymbol{q}^2 + \frac{3(5k_{\rm F1}+3m\alpha)}{32mk_{\rm F1}(k_{\rm F1}+m\alpha)}B_y q_x\boldsymbol{q}^2 + O(\boldsymbol{q}^4), \quad \text{(A9)}$$

$$\langle\Omega(\boldsymbol{k},\boldsymbol{q})^4\rangle = O(\boldsymbol{q}^4). \quad \text{(A10)}$$

This result is reasonable because the third-order term in the momentum vanishes for $m\to\infty$. The case of the valence band ($E_{\rm F}<0$) can be obtained in a similar manner, and we can show that the free energy is obtained by replacing α with $-\alpha$, B_y with $-B_y$, $k_{\rm F1}=-m\alpha+\sqrt{mE_{\rm FR}}$ with $k_{\rm F2}=m\alpha-\sqrt{mE_{\rm FR}}$, and $\nu_1=\frac{m}{2\pi}(1-\alpha\sqrt{m/E_{\rm FR}})$ with $\nu_2=\frac{m}{2\pi}(-1+\alpha\sqrt{m/E_{\rm FR}})$. We can also derive the GL free energy for the model with the hexagonal warping [Eq. (50)] in the same way.

APPENDIX B: IMPURITY EFFECT IN TMD

The effect of superconducting fluctuation is more prominent for dirty samples according to the Ginzburg-Levanyuk criterion [13]

$$|\epsilon|\lesssim\left[\frac{k_{\rm F}\xi_0}{(k_{\rm F}\xi)^D}\right]^{\frac{2}{4-D}}, \quad \text{(B1)}$$

where D is the dimension of the system, $\epsilon=(T-T_0)/T_0$, and $\xi_0\sim v_{\rm F}/T_0$. ξ is the coherence length for either clean or dirty samples. Here, we consider the impurity effect on the GL equation with $\boldsymbol{q}$-cubic term originating from trigonal warping for MoS_2. To deal with the impurities, we take quasiclassical Green function method [29]. We introduce the normal and anomalous quasiclassical Green functions by $g(\hat{\boldsymbol{k}},i\omega_n;\boldsymbol{r})$ and $f(\hat{\boldsymbol{k}},i\omega_n;\boldsymbol{r})$, respectively, where $\hat{\boldsymbol{k}}$ is the unit vector in the direction of $\boldsymbol{k}$ on the warped Fermi surface. The gap equation is given by

$$\Delta(\boldsymbol{r}) = \pi i\nu V^{\rm g}T\sum_n\langle f(\hat{\boldsymbol{k}},i\omega_n;\boldsymbol{r})\rangle_{\boldsymbol{k}}, \quad \text{(B2)}$$

where the angle brackets mean the average with respect to $\boldsymbol{k}$. $V^{\rm g}$ and ν are the attractive interaction parameter and density of states at the Fermi level, respectively. To derive the GL theory, we expand the right-hand side of Eq. (B2). The terms without spatial derivatives are not affected by impurities, which is known as the Anderson theorem. Hence, we only keep the linear term in Δ and consider spatial derivatives. With this condition we can use $g(\hat{\boldsymbol{k}},i\omega_n;\boldsymbol{r})=\operatorname{sgn}\omega_n$, since it does not have the linear term of Δ. The anomalous Green function is described by the Eilenberger equation

$$i\boldsymbol{v}_{\rm F}(\hat{\boldsymbol{k}})\cdot\nabla f+2i\omega_n f-2\Delta g+\frac{i}{\tau}(\langle g\rangle_{\boldsymbol{k}}f-\langle f\rangle_{\boldsymbol{k}}g)=0, \quad \text{(B3)}$$

where $\boldsymbol{v}_{\rm F}$ is the Fermi velocity and τ is the relaxation time. The self-energy from impurities has been included by the self-consistent Born approximation. The Zeeman energy can be accounted for by the simple replacement $i\omega_n\to i\omega_n+B_z$, and we do not write this explicitly for the moment. Now, we perform the gradient expansion as $f=f_0+f_1+f_2+f_3+\cdots$. The zeroth- and first-order terms can be explicitly written as

$$\langle f_0\rangle_{\boldsymbol{k}} = f_0 = \frac{\Delta\operatorname{sgn}\omega_n}{i\omega_n}, \quad \text{(B4)}$$

$$\langle f_1\rangle_{\boldsymbol{k}} = -\frac{i\langle\boldsymbol{v}_{\rm F}\rangle_{\boldsymbol{k}}\cdot\nabla f_0}{2i\omega_n}, \quad \text{(B5)}$$

where $\tilde{\omega}_n=\omega_n+\frac{1}{2\tau}\operatorname{sgn}\omega_n$. We conclude $\langle f_1\rangle_{\boldsymbol{k}}=0$ since $\langle\boldsymbol{v}_{\rm F}\rangle_{\boldsymbol{k}}=\boldsymbol{0}$ is satisfied. The higher-order terms can also be derived as

$$\langle f_2\rangle_{\boldsymbol{k}} = \frac{\langle(i\boldsymbol{v}_{\rm F}\cdot\nabla)^2 f_0\rangle_{\boldsymbol{k}}}{4i\omega_n i\tilde{\omega}_n}, \quad \text{(B6)}$$

$$\langle f_3\rangle_{\boldsymbol{k}} = -\frac{\langle(i\boldsymbol{v}_{\rm F}\cdot\nabla)^3 f_0\rangle_{\boldsymbol{k}}}{4i\omega_n(i\tilde{\omega}_n)^2}. \quad \text{(B7)}$$

$\langle f_3\rangle_{\boldsymbol{k}}$ can be finite if the system has a trigonal warping. To be compatible with the results in TMD, there are the relations

$$\langle(i\boldsymbol{v}_{\rm F}\cdot\nabla)^2\rangle_{\boldsymbol{k}} = C_2\nabla^2, \quad \text{(B8)}$$

$$\langle(i\boldsymbol{v}_{\rm F}\cdot\nabla)^3\rangle_{\boldsymbol{k}} = iC_3\partial_x\left(\partial_x^2-3\partial_y^2\right). \quad \text{(B9)}$$

The real constants C_2 and C_3 are determined to be consistent with the expressions in the clean limit which has already been obtained in Ref. [10].

We now replace $i\omega_n$ by $i\omega_n+B_z$ to include the Zeeman energy, and take the lowest-order contribution of the external magnetic field B_z. We substitute these expressions into the gap equation. The coefficient $\gamma(\tau)$ of $\boldsymbol{q}$-square term and $K(\tau)$ of $\boldsymbol{q}$-cubic term in the GL free energy (92), which are now dependent on the mean-free time τ, are given by

$$\gamma(\tau)/\gamma(\infty) = \sum_n\frac{1}{|\omega_n|^2\left(|\omega_n|+\frac{1}{2\tau}\right)}\Bigg/\sum_n\frac{1}{|\omega_n|^3}, \quad \text{(B10)}$$

$$K(\tau)/K(\infty) = \frac{1}{2}\sum_n\frac{1}{|\omega_n|^2\left(|\omega_n|+\frac{1}{2\tau}\right)^2}\times\left(\frac{1}{|\omega_n|}+\frac{1}{|\omega_n|+\frac{1}{2\tau}}\right)\Bigg/\sum_n\frac{1}{|\omega_n|^5}. \quad \text{(B11)}$$

These results can be used at any purity of samples and go to unity for the clean limit. The $\boldsymbol{q}$-square coefficient here is not a new result which can be seen in, e.g., Ref. [43], but the $\boldsymbol{q}$-cubic coefficient is first derived. Particularly for the γ value, the ratio between dirty ($\tau T_0\ll 1$) and clean ($\tau T_0\gg 1$) limits is given using Eq. (60) by

$$\frac{\gamma^{\rm f}_{\rm S,dirty}}{\gamma^{\rm f}_{\rm S,clean}}\sim\tau T_0 \quad \text{(B12)}$$

for superconducting fluctuation contribution. For vortex flow contribution, on the other hand, the transport coefficients are dependent on σ_n ($\simeq n_e e^2\tau/m$) and cannot be written in a simple way, but can be in general estimated from the above information.

APPENDIX C: EFFECT OF LANDAU LEVEL FOR PARACONDUCTIVITY IN TMD

1. Formulation

We here extend the calculation for the paraconductivity in the low-field limit to the case in the presence of quartic term and magnetic field. The paraconductivity from superconducting fluctuations can be evaluated at arbitrary strength of the magnetic field by considering the Landau levels. Let us begin with the GL free energy

$$F = \int d^2\boldsymbol{r}\, \Psi^* \left[a + \frac{\boldsymbol{P}^2}{2m^*} + \Lambda B_z \left(P_x^3 - 3\overline{P_x P_y^2} \right) \right] \Psi, \quad \text{(C1)}$$

where $\boldsymbol{P} = -i\nabla - e^*\boldsymbol{A}$ with $e^* = 2e$ and $m^* = 2m$. The quartic term with $|\Psi|^4$ can be effectively included in the square term by using the self-consistent harmonic approximation and is dropped here. We will explain this point later. The spatially averaged supercurrent is given in the simple form

$$J_{sx} = -|e^*| \int \frac{d^2\boldsymbol{r}}{\Omega} \Psi^* \left[\frac{1}{m^*} P_x + 3\Lambda B_z \left(P_x^2 - P_y^2 \right) \right] \Psi, \quad \text{(C2)}$$

where $\Omega = \int d^2\boldsymbol{r}\, 1$ is a two-dimensional system volume. The y component can be constructed by symmetry and we do not consider here. We choose the vector potential as $A_x = -E_x t$ and $A_y = -E_y t + B_z x$. Now, we expand the complex function Ψ as

$$\Psi(\boldsymbol{r}, t) = \sum_{kn} c_{kn}(t) e^{-iky} e^{i|e|E_x t[x - x_{0k}(t/2)]} h_n[x - x_{0k}(t)], \quad \text{(C3)}$$

$$x_{0k}(t) = \frac{k + |e^*|E_y t}{|e^*|B_z}, \quad \text{(C4)}$$

where $h_n(x)$ is an eigenfunction of the one-dimensional harmonic oscillator with the quantum number n. We can show the following relations:

$$P_x \Psi = -i\sqrt{\frac{m^*\omega}{2}} (b - b^\dagger)\Psi, \quad \text{(C5)}$$

$$\frac{\boldsymbol{P}^2}{2m} \Psi = \omega \left(b^\dagger b + \frac{1}{2} \right) \Psi, \quad \text{(C6)}$$

$$\left(P_x^3 - 3\overline{P_x P_y^2} \right) \Psi = 4i \left(\frac{m^*\omega}{2} \right)^{3/2} (b^3 - b^{\dagger 3}) \Psi, \quad \text{(C7)}$$

$$\left(P_x^2 - P_y^2 \right) \Psi = -m^*\omega (b^2 + b^{\dagger 2}) \Psi, \quad \text{(C8)}$$

with $\omega = |e^*|B_z/m^*$ being a cyclotron frequency. We have used the relations

$$\partial_x h_n(x) = \sqrt{\frac{m^*\omega}{2}} (b - b^\dagger) h_n(x), \quad \text{(C9)}$$

$$x h_n(x) = \sqrt{\frac{1}{2m^*\omega}} (b + b^\dagger) h_n(x). \quad \text{(C10)}$$

The operators b and $b^\dagger$ act only on h_n as

$$b h_n = \sqrt{n} h_{n-1}, \quad \text{(C11)}$$

$$b^\dagger h_n = \sqrt{n+1} h_{n+1}. \quad \text{(C12)}$$

Let us consider the TDGL equation in the presence of thermal fluctuations:

$$-\Gamma \partial_t \Psi = \frac{\delta F}{\delta \Psi^*} - f. \quad \text{(C13)}$$

We note that Γ here is different from the one in Eq. (91) by a constant factor. Equation (C13) can be rewritten in terms of $c_{kn}(t)$ as

$$\begin{aligned} -\Gamma \partial_t c_n = & \left[a + \omega \left(n + \frac{1}{2} \right) \right] c_n - f_n' \\ & + 4i\Lambda B_z \left(\frac{m^*\omega}{2} \right)^{3/2} [\sqrt{{}_{n+3}\mathrm{P}_3}\, c_{n+3} - \sqrt{{}_n\mathrm{P}_3}\, c_{n-3}] \\ & + \frac{i|e|\Gamma}{\sqrt{2m^*\omega}} [\sqrt{n+1} E c_{n+1} + \sqrt{n} E^* c_{n-1}], \end{aligned} \quad \text{(C14)}$$

where we have defined the complex electric field $E = E_x + iE_y$ and have omitted k. The symbol ${}_n\mathrm{P}_m = n!/(n-m)!$ is the permutation. This equation can be solved perturbatively. We expand the solution as

$$c_n(t) = \sum_{p,q=0}^{\infty} c_n^{pq}(t), \quad \text{(C15)}$$

where c_n^{pq} is a contribution of $O(E^p \Lambda^q)$, and each term satisfies the following recursive equation:

$$\begin{aligned} c_n^{pq}(t) = \frac{i}{\Gamma} \int_{-\infty}^{t} dt' \big[& \beta \left(\sqrt{{}_{n+3}\mathrm{P}_3}\, c_{n+3}^{p,q-1} - \sqrt{{}_n\mathrm{P}_3}\, c_{n-3}^{p,q-1} \right) \\ & + \alpha \left(\sqrt{n+1} E c_{n+1}^{p-1,q} + \sqrt{n} E^* c_{n-1}^{p-1,q} \right) \big] e^{(t'-t)A_n}. \end{aligned} \quad \text{(C16)}$$

Here, we have defined

$$\alpha = -\frac{|e|\Gamma}{\sqrt{2m^*\omega}}, \quad \beta = -4\Lambda B_z \left(\frac{m^*\omega}{2} \right)^{3/2}, \quad \text{(C17)}$$

$$A_n = \frac{a + \omega\left(n + \frac{1}{2}\right)}{\Gamma}, \quad \text{(C18)}$$

to make the notation simple.

We rewrite the current along x direction as

$$\begin{aligned} J_{sx} = \frac{|e^*|^2 B_z}{\pi} \sum_{n=0}^{E_c/\omega} \Bigg[& \sqrt{\frac{\omega}{2m^*}} \sqrt{n+1}\, \mathrm{Im}\, \langle c_{n+1}^* c_n \rangle \\ & + 3\Lambda B_z m^* \omega \sqrt{{}_{n+2}\mathrm{P}_2}\, \mathrm{Re}\, \langle c_{n+2}^* c_n \rangle \Bigg], \end{aligned} \quad \text{(C19)}$$

where we have used the relation for the number of degeneracy:

$$\sum_k 1 = \frac{\Omega}{2\pi \ell_B^2} \quad \text{(C20)}$$

with $\ell_B = \sqrt{1/|e^*|B_z}$ being the magnetic length. The cutoff energy is given by $E_c \sim T_0$.

2. Evaluation of current

We first consider the zeroth-order component:

$$\left\langle c_n^{00*}(t_1)c_n^{00}(t_2)\right\rangle = \frac{T/\Gamma}{A_n}e^{-|t_1-t_2|A_n}. \tag{C21}$$

To evaluate the current we need only the equal-time component of the forms $\langle c^*_{n+1}c_n\rangle$ and $\langle c^*_{n+2}c_n\rangle$. The $O(E^1)$ components are calculated from Eqs. (C16) and (C21) as

$$\left\langle c_{n+1}^{10*}c_n^{00}\right\rangle = -\frac{i\alpha ET}{\Gamma^2}\sqrt{n+1}\frac{1}{A_n(A_n+A_{n+1})}, \tag{C22}$$

$$\left\langle c_{n-1}^{10*}c_n^{00}\right\rangle = -\frac{i\alpha E^*T}{\Gamma^2}\sqrt{n}\frac{1}{A_n(A_n+A_{n-1})}. \tag{C23}$$

The $O(E^2)$ components are calculated as

$$\left\langle c_{n+2}^{10*}c_n^{10}\right\rangle = \frac{\alpha^2E^2T}{\Gamma^3}\sqrt{{}_{n+2}\mathrm{P}_2}\,H_1(n+1,n+2,n), \tag{C24}$$

$$\left\langle c_{n+2}^{00*}c_n^{20}\right\rangle = \frac{-\alpha^2E^2T}{\Gamma^3}\sqrt{{}_{n+2}\mathrm{P}_2}\,H_2(n+2,n,n+1), \tag{C25}$$

$$\left\langle c_{n-2}^{00*}c_n^{20}\right\rangle = \frac{-\alpha^2(E^*)^2T}{\Gamma^3}\sqrt{{}_{n}\mathrm{P}_2}\,H_2(n-2,n,n-1), \tag{C26}$$

where

$$H_1(i,j,k) = \frac{1}{A_i(A_j+A_k)}\left[\frac{1}{A_i+A_k}+\frac{1}{A_i+A_j}\right], \tag{C27}$$

$$H_2(i,j,k) = \frac{1}{A_i(A_i+A_k)(A_i+A_j)}. \tag{C28}$$

The $O(E^2\Lambda^1)$ components are also calculated as

$$\left\langle c_{n+1}^{11*}c_n^{10}\right\rangle = -(C^{21})^*\left[\frac{{}_{n+1}\mathrm{P}_3}{\sqrt{n+1}}F_1(n-1,n+1,n,n-2)+\frac{{}_{n+2}\mathrm{P}_3}{\sqrt{n+1}}F_1(n-1,n+1,n,n+2)\right], \tag{C29}$$

$$\left\langle c_{n-1}^{11*}c_n^{10}\right\rangle = -C^{21}\left[\frac{{}_{n+2}\mathrm{P}_3}{\sqrt{n}}F_1(n+1,n-1,n,n+2)+\frac{{}_{n+1}\mathrm{P}_3}{\sqrt{n}}F_1(n+1,n-1,n,n-2)\right], \tag{C30}$$

$$\left\langle c_{n+1}^{20*}c_n^{01}\right\rangle = (C^{21})^*\frac{{}_{n+3}\mathrm{P}_3}{\sqrt{n+1}}F_1(n+3,n+1,n,n+2), \tag{C31}$$

$$\left\langle c_{n-1}^{20*}c_n^{01}\right\rangle = C^{21}\frac{{}_{n}\mathrm{P}_3}{\sqrt{n}}F_1(n-3,n-1,n,n-2), \tag{C32}$$

$$\begin{aligned}\left\langle c_{n+1}^{21*}c_n^{00}\right\rangle = (C^{21})^*\Bigg[&\frac{{}_{n+1}\mathrm{P}_3}{\sqrt{n+1}}F_2(n,n+1,n-2,n-1)+\frac{{}_{n+3}\mathrm{P}_3}{\sqrt{n+1}}F_2(n,n+1,n+2,n+3)\\&+\frac{{}_{n+2}\mathrm{P}_3}{\sqrt{n+1}}F_2(n,n+1,n+2,n-1)\Bigg],\end{aligned} \tag{C33}$$

$$\left\langle c_{n-1}^{21*}c_n^{00}\right\rangle = C^{21}\left[\frac{{}_{n+2}\mathrm{P}_3}{\sqrt{n}}F_2(n,n-1,n+2,n+1)\frac{{}_{n}\mathrm{P}_3}{\sqrt{n}}F_2(n,n-1,n-2,n-3)\frac{{}_{n+1}\mathrm{P}_3}{\sqrt{n}}F_2(n,n-1,n-2,n+1)\right], \tag{C34}$$

where we have defined the complex constant by $C^{21} = i\alpha^2\beta E^2T/\Gamma^4$ and the functions $F_{1,2}$ by

$$F_1(i,j,k,l) = \frac{1}{A_i(A_j+A_k)}\left[\frac{1}{(A_i+A_l)(A_k+A_l)}+\frac{1}{(A_i+A_k)(A_k+A_l)}+\frac{1}{(A_i+A_l)(A_i+A_j)}\right], \tag{C35}$$

$$F_2(i,j,k,l) = \frac{1}{A_i(A_i+A_l)(A_i+A_k)(A_i+A_j)}. \tag{C36}$$

The quantities other than those listed above can be evaluated using complex-conjugation relations. Substituting the above expressions into the current, we obtain the linear and nonlinear paraconductivities. We define the transport coefficients by $J_{sx} = \sigma_1E_x + \sigma_2(E_x^2 - E_y^2) + O(E^3)$ and each coefficient is given by

$$\sigma_1 = \frac{|e^*|^2\omega T}{2\pi\Gamma}\sum_n\frac{n+1}{A_n+A_{n+1}}\left(\frac{1}{A_n}-\frac{1}{A_{n+1}}\right), \tag{C37}$$

$$\sigma_2 = -\frac{|e^*|^3m^*\Lambda B_z\omega T}{2\pi\Gamma^2}\sum_n[\omega X(n)+3\Gamma Y(n)], \tag{C38}$$

where

$$\begin{aligned} X(n) =& {}_{n+1}\mathrm{P}_3 F_1(n-1, n+1, n, n-2) \\ &+ {}_{n+2}\mathrm{P}_3 F_1(n-1, n+1, n, n+2) \\ &+ {}_{n+3}\mathrm{P}_3 F_1(n+2, n, n+1, n+3) \\ &+ {}_{n+2}\mathrm{P}_3 F_1(n+2, n, n+1, n-1) \\ &- {}_{n+3}\mathrm{P}_3 F_1(n+3, n+1, n, n+2) \\ &- {}_{n+1}\mathrm{P}_3 F_1(n-2, n, n+1, n-1) \\ &- {}_{n+1}\mathrm{P}_3 F_2(n, n+1, n-2, n-1) \\ &- {}_{n+3}\mathrm{P}_3 F_2(n, n+1, n+2, n+3) \\ &- {}_{n+2}\mathrm{P}_3 F_2(n, n+1, n+2, n-1) \\ &- {}_{n+3}\mathrm{P}_3 F_2(n+1, n, n+3, n+2) \\ &- {}_{n+1}\mathrm{P}_3 F_2(n+1, n, n-1, n-2) \\ &- {}_{n+2}\mathrm{P}_3 F_2(n+1, n, n-1, n+2), \end{aligned} \tag{C39}$$

$$\begin{aligned} Y(n) =& {}_{n+2}\mathrm{P}_2[H_2(n+2, n, n+1) + H_2(n, n+2, n+1) \\ &- H_1(n+1, n+2, n)]. \end{aligned} \tag{C40}$$

One can check that the function in the n summation behaves as $O(n^{-2})$ or faster at large n, so we do not need the cutoff for convergence. The ordinary paraconductivity σ_1 here reproduces the results derived in the previous work [44].

3. Effect of quartic term

Here, we consider the quartic term in GL free energy

$$F_4 = \frac{b}{2} \int d^2\boldsymbol{r}\, |\Psi|^4. \tag{C41}$$

We use the self-consistent harmonic approximation [45]

$$|\Psi|^4 = \Psi^*\Psi^*\Psi\Psi \simeq 2\langle|\Psi|^2\rangle|\Psi|^2. \tag{C42}$$

Hence, the coefficient a is replaced by $a' = a + b\langle|\Psi|^2\rangle$. We have the self-consistent equation to determine a':

$$\langle|\Psi|^2\rangle = \frac{1}{\Omega}\sum_{kn}\langle|c_{kn}|^2\rangle = \frac{m^*T}{2\pi}\sum_{n=0}^{E_c/\omega}\frac{1}{n+\frac{1}{2}+\frac{a+b\langle|\Psi|^2\rangle}{\omega}}. \tag{C43}$$

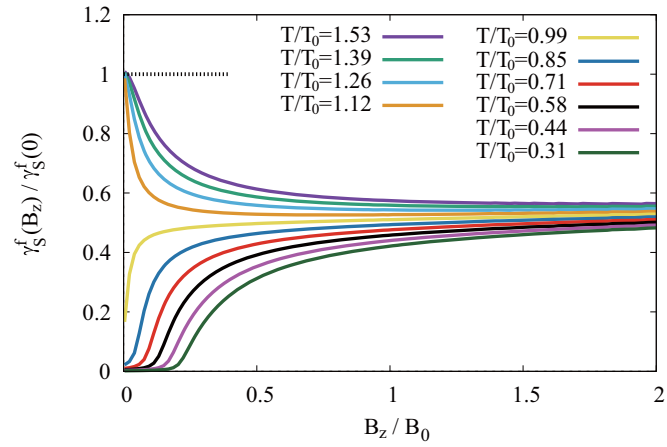

FIG. 5. Magnetic field B_z dependence of the γ value from paraconductivity. The unit for the magnetic field is $B_0 = m^*T_0/|e^*|$. The parameters are chosen as $a(T) = 0.02(T - T_0)$, $bm^* = 0.005$, and $E_c = 4T_0$. Note that the normal conductivity is neglected.

Note that here we need the cutoff energy $E_c \sim T_0$ for convergence, and have neglected the $\boldsymbol{P}$-cubic term which is irrelevant in the leading-order contribution for the equilibrium case. With this consideration, the finite transition temperature in mean field theory is washed away in the two-dimensional system reflecting the Mermin-Wagner theorem.

Figure 5 shows the exemplary results for the magnetic field dependence of $\gamma_S(B_z) = \sigma_2/\sigma_1^2 B_z W$ which is normalized by the value at $B_z = 0$. Above the mean field transition temperature T_0, the γ value decreases with increasing B_z, and it becomes nearly half at high fields. On the contrary, below T_0, the γ value is small at low B_z and increases by applying magnetic field. Although $\gamma_S(B_z)/\gamma_S(0)$ goes to 1 at zero field, the corresponding B_z range is so narrow that such regime (i.e., $a' \gg \omega$) cannot be seen practically. This is because the value of a' for $T < T_0$ remains positive but is so tiny, and therefore the behavior is very sensitive to the small value of B_z. We note that in actual systems the component of normal conductivity is also finite and modifies the γ value down to zero at high magnetic fields.

[1] L. Onsager, Reciprocal relations in irreversible processes. I, Phys. Rev. **37**, 405 (1931).

[2] R. Kubo, Statistical-mechanical theory of irreversible processes. I. General theory and simple applications to magnetic and conduction problems, J. Phys. Soc. Jpn. **12**, 570 (1957).

[3] G. L. J. A. Rikken, J. Fölling, and P. Wyder, Electrical Magnetochiral Anisotropy, Phys. Rev. Lett. **87**, 236602 (2001).

[4] T. Morimoto and N. Nagaosa, Chiral Anomaly and Giant Magnetochiral Anisotropy in Noncentrosymmetric Weyl Semimetals, Phys. Rev. Lett. **117**, 146603 (2016).

[5] G. L. J. A. Rikken and E. Raupach, Observation of magnetochiral dichroism, Nature (London) **390**, 493 (1997).

[6] V. Krstić, S. Roth, M. Burghard, K. Kern, and G. L. J. A. Rikken, Magneto-chiral anisotropy in charge transport through single-walled carbon nanotubes, J. Chem. Phys. **117**, 11315 (2002).

[7] G. L. J. A. Rikken and P. Wyder, Magnetoelectric Anisotropy in Diffusive Transport, Phys. Rev. Lett. **94**, 016601 (2005).

[8] F. Pop, P. Auban-Senzier, E. Canadell, G. L. J. A. Rikken, and N. Avarvari, Electrical magnetochiral anisotropy in a bulk chiral molecular conductor, Nat. Commun. **5**, 3757 (2014).

[9] T. Ideue, K. Hamamoto, S. Koshikawa, M. Ezawa, S. Shimizu, Y. Kaneko, Y. Tokura, N. Nagaosa, and Y. Iwasa, Bulk rectification effect in a polar semiconductor, Nat. Phys. **13**, 578 (2017).

[10] R. Wakatsuki, Y. Saito, S. Hoshino, Y. M. Itahashi, T. Ideue, M. Ezawa, Y. Iwasa, and N. Nagaosa, Nonreciprocal charge transport in noncentrosymmetric superconductors, Sci. Adv. **3**, e1602390 (2017).

[11] B. I. Halperin and D. R. Nelson, Resistive transition in superconducting films, J. Low Temp. Phys. **36**, 599 (1979).

[12] W. J. Skocpol and M. Tinkham, Fluctuations near superconducting phase transitions, Rep. Prog. Phys. **38**, 1049 (1975).

[13] A. I. Larkin and A. A. Varlamov, in *Fluctuation Phenomena in Superconductors* (Springer, Berlin, 2008), pp. 369–458.

[14] L. G. Aslamazov and A. I. Larkin, Effect of fluctuations on the properties of a superconductor above the critical temperature, Fiz. Tverd. Tela, **10**, 1104 (1968) [Sov. Phys.–Solid State **10**, 875 (1968)].

[15] K. Maki, Critical fluctuation of the order parameter in a superconductor. I, Prog. Theor. Phys. **40**, 193 (1968).

[16] R. S. Thompson, Microwave, flux flow, and flucutuation resistance of dirty type-II superconductors, Phys. Rev. B **1**, 327 (1970).

[17] A. Schmid, Diamagnetic susceptibility at the transition to the superconducting state, Phys. Rev. **180**, 527 (1969).

[18] R. Wakatsuki and N. Nagaosa, Nonreciprocal Current in Noncentrosymmetric Rashba Superconductors, Phys. Rev. Lett. **121**, 026601 (2018).

[19] S.-K. Yip, Fluctuations in an impure unconventional superconductor, Phys. Rev. B **41**, 2612 (1990).

[20] *Non-Centrosymmetric Superconductors*, edited by E. Bauer and M. Sigrist (Springer, Berlin, 2012).

[21] S. Yip, Noncentrosymmetric superconductors, Annu. Rev. Condens. Matter Phys. **5**, 15 (2014).

[22] L. Fu, Hexagonal Warping Effects in the Surface States of the Topological Insulator Bi_2Te_3, Phys. Rev. Lett. **103**, 266801 (2009).

[23] D. R. Nelson and J. M. Kosterlitz, Universal Jump in the Superfluid Density of Two-Dimensional Superfluids, Phys. Rev. Lett. **39**, 1201 (1977).

[24] J. M. Kosterlitz, The critical properties of the two-dimensional xy model, J. Phys. C: Solid State Phys. **7**, 1046 (1974).

[25] M. Tinkham, *Introduction to Superconductivity* (McGraw-Hill, New York, 1996).

[26] J. Bardeen and M. J. Stephen, Theory o the motion of vortices in superconductors, Phys. Rev. **140**, A1197 (1965).

[27] P. Nozières and W. F. Vinen, The motion of flux lines in type II superconductors, Philos. Mag. **14**, 667 (1966)

[28] A. Schmid, A time dependent Ginzburg-Landau eequation and its application to the problem of resistivity in the mixed state, Phys. Kondens. Mater. **5**, 302 (1966).

[29] N. B. Kopnin, *Theory of Nonequilibrium Superconductivity* (Oxford University Press, Oxford, 2001).

[30] J. Pearl, Current distribution in superconducting films carrying quantized fluxoids, Appl. Phys. Lett. **5**, 65 (1964).

[31] Y. Kato and C.-K. Chung, Nature of driving force on an isolated moving vortex in dirty superconductors, J. Phys. Soc. Jpn. **85**, 033703 (2016).

[32] C.-S. Lee, B. Jankó, I. Derény, and A.-L. Barabási, Reducing vortex density in superconductors using the 'ratchet' effect, Nature (London) **400**, 337 (1999).

[33] J. E. Villegas, S. Savel'ev, F. Nori, E. M. Gonzalez, J. V. Anguita, R. García, and J. L. Vicent, A Superconducting reversible rectifier that controls the motion of magnetic flux quanta, Science **302**, 1188 (2003).

[34] J. E. Villegas, E. M. Gonzalez, M. P. Gonzalez, J. V. Anguita, and J. L. Vicent, Experimental ratchet effect in superconducting films with periodic arrays of asymmetric potentials, Phys. Rev. B **71**, 024519 (2005).

[35] Y. Saito *et al.* (private communication).

[36] P. Reimann, C. Van den Broeck, H. Linke, P. Hänggi, J. M. Rubi, and A. Pérez-Madrid, Giant Acceleration of Free Diffusion by Use of Tilted Periodic Potentials, Phys. Rev. Lett. **87**, 010602 (2001).

[37] N. Reyren, S. Thiel, A. D. Caviglia, L. F. Kourkoutis, G. Hammerl, C. Richter, C. W. Schneider, T. Kopp, A.-S. Rüetschi, D. Jaccard, M. Gabay, D. A. Muller, J.-M. Triscone, and J. Mannhart, Superconducting interfaces between insulating oxides, Science **317**, 1196 (2007).

[38] A. D. Caviglia, S. Gariglio, N. Reyren, D. Jaccard, T. Schneider, M. Gabay, S. Thiel, G. Hammerl, J. Mannhart, and J.-M. Triscone, Electric field control of the $LaAlO_3/SrTiO_3$ interface ground state, Nature (London) **456**, 624 (2008).

[39] G. Herranz, G. Singh, N. Bergeal, A. Jouan, J. Lesueur, J. Gázquez, M. Varela, M. Scigaj, N. Dix, F. Sánchez, and J. Fontcuberta, Engineering two-dimensional superconductivity and Rashba spin-orbit coupling in $LaAlO_3/SrTiO_3$ quantum wells by selective orbital occupancy, Nat. Commun. **6**, 6028 (2015).

[40] E. Maniv, M. B. Shalom, A. Ron, M. Mograbi, A. Palevski, M. Goldstein, and Y. Dagan, Strong correlations elucidate the electronic structure and phase diagram of $LaAlO_3/SrTiO_3$ interface, Nat. Commun. **6**, 8239 (2015).

[41] K. W. Kim, T. Morimoto, and N. Nagaosa, Shift charge and spin photocurrents in Dirac surface states of topological insulator, Phys. Rev. B **95**, 035134 (2017).

[42] Y. Saito, Y. Nakamura, M. S. Bahramy, Y. Kohama, J. Ye, Y. Kasahara, Y. Nakagawa, M. Onga, M. Tokunaga, T. Nojima, Y. Yanase, and Y. Iwasa, Superconductivity protected by spin-valley locking in ion-gated MoS_2, Nat. Phys. **12**, 144 (2016).

[43] Y. B. Kim and M. J. Stephen, in *Superconductivity*, edited by R. D. Parks (Marcel Dekker, New York, 1969).

[44] E. Abrahams, R. E. Prange, and M. J. Stephen, Effect of a magnetic field on fluctuations above Tc, Physica (Amsterdam) **55**, 230 (1971).

[45] See, for example, P. M. Chaikin and T. C. Lubensky, *Principles of Condensed Matter Physics* (Cambridge University Press, New York, 1995).